IEEE Access
Multidisciplinary | Rapid Review | Open Access Journal

Received July 3, 2019, accepted July 19, 2019, date of publication July 31, 2019, date of current version August 16, 2019.

Digital Object Identifier 10.1109/ACCESS.2019.2932118

Vibration Test of Single Coal Gangue Particle Directly Impacting the Metal Plate and the Study of Coal Gangue Recognition Based on Vibration Signal and Stacking Integration

YANG YANG[1], QINGLIANG ZENG[1,2], GUANGJUN YIN[1], AND LIRONG WAN[1]
[1]College of Mechanical and Electronic Engineering, Shandong University of Science and Technology, Qingdao 266590, China
[2]College of Information Science and Engineering, Shandong Normal University, Jinan 250358, China

Corresponding author: Qingliang Zeng (qlzeng@sdust.edu.cn)

This work was supported in part by the Postgraduate Science and Technology Innovation Project of Shandong University of Science and Technology under Grant SDKDYC190108, in part by the National Natural Science Fund of China under Grant 51674155, in part by the Innovative Team Development Project of Ministry of Education under Grant IRT_16R45, in part by the Special funds for Climbing Project of Taishan Scholars, and in part by the National Natural Science Fund of Shandong Province under Grant ZR2019MEE067.

ABSTRACT In order to realize the recognition of coal gangue in the top coal caving process, a scheme of the coal gangue recognition based on the collision vibration signal between coal gangue and the metal plate is proposed in this paper, a systematic and standardized impacting test between coal gangue particles and the metal plate is designed for the first time, the vibration signal standardized processing method by the signal intercepting and the coal gangue impact vibration signal recognition algorithm by stacking integration are innovatively proposed. First, a single particle impact on the metal plate test-bed was designed and constructed. Then 1,000 groups coal and 1,000 groups gangue impact on the metal plate tests were carried out respectively, and the vibration acceleration signals of the metal plate were collected. After that, through the signal intercepting, calculating the time-domain characteristics and HHT processing of the vibration signal, 10 time-frequency characteristics, such as the variance of the intercepted signal and the Hilbert marginal spectrum energy value, are determined to form the feature vector. Finally, based on the two different type of the signal samples, the intercepted signal feature vector, and the original intercepted signal, coal gangue recognition by the seven machine learning algorithms, including the decision tree (DT), random forest (RF), XGBoost, long short-term memory (LSTM), support vector machine (SVM), factorization machine (FM), and stacking integration is carried out respectively, and the basis for selecting recognition schemes is discussed. The results show that the coal gangue recognition rate with the same recognition algorithm by using the intercepted signal samples is higher than that of the feature vector samples, the Staking integration algorithm based on the same sample has the highest recognition rate, and the Staking integration algorithm based on the feature vector has the most significant comprehensive advantage in top coal caving process.

INDEX TERMS Coal gangue recognition, EMD, impact, intercepted signal, stacking integration algorithm, vibration signal.

I. INTRODUCTION

Coal which has dual attributes of energy and resources is the main energy source in China [1]–[3]. Among them, thick coal seams account for a large proportion of proven coal reserves and production in China. As shown in Figure 1, comprehensive mechanized caving mining technology [4]–[10] has been widely used in the mining of thick and extra-thick coal seams in China with its characteristics of high production, high efficiency, low energy consumption and low investment. However, in the actual production process, there is large manpower investment, and the working face environment is extremely bad. Also artificial judgment of the degree of top coal caving will inevitably lead to the situation of Under-caving and Over-caving, thus resulting in the reduction of coal recovery rate or transportation cost increase and coal quality decline and other problems. The realization of unmanned automation technology for fully

The associate editor coordinating the review of this manuscript and approving it for publication was Jingchang Huang.

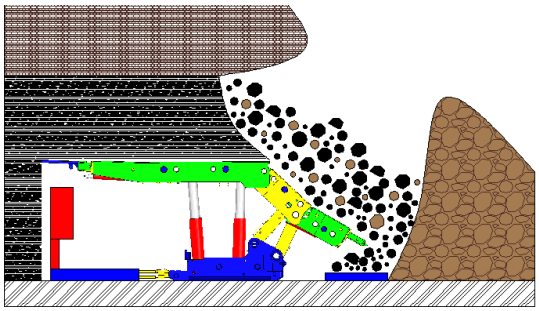

FIGURE 1. Top coal caving.

mechanized top coal mining can release manpower, improve production safety and efficiency, and reduce coal mining cost. In order to realize the unmanned automation of the fully mechanized caving, the ''bottleneck'' problem of coal gangue recognition in top coal caving [11], [12] must be solved first.

At present, methods of coal gangue identification (or sorting) mainly include image recognition, cutting force recognition, laser scanning separation, vibration recognition and voice recognition. Liu et al. established the coal gangue automatically sorts supervisory system by adopting technology of image processing and pattern recognition to identify and sort gangue [13]. Sun and She [14], [16] carried out the coal rock image decomposition, feature extraction and recognition by Daubechies wavelet and identify coal and gangue base on SVM and image texture features. Hou *et al.* established a coal gangue automation selection system based on the difference of coal gangue surface texture features and gray features, and combined image feature extraction with artificial neural network for coal gangue identification, so as to realize automatic coal and gangue separation [17]. Wang and Zhang [18] proposed a three-dimensional laser scanning separation method for coal gangue based on density, the mathematical model for coal gangue recognition was established, and an algorithm for the recognition threshold and recognition rate was proposed. He presented a new method based on sparse representation for coal and gangue signal recognition [19]. Based on the fractal model of impact crushing probability, Liu *et al.* carried out impact crushing experiments on gangue particles in three mines, and compared the results with those of impact crushing experiments of coal particles in the same mines, which provided favorable conditions for the separation of coal and gangue by impact crushing [20]. Zhou *et al.* proved that the crushing probability of coal and gangue increases with the increase of impact velocity through the impact crushing test of coal gangue, but the crushing probability of the gangue in the same condition is far less than that of coal, which provides a research foundation for coal gangue recognition based on impact [21]. Liu Wei *et al.* proposed a new coal gangue interface recognition method based on vibration signal analysis, which extracted vibration characteristics based on Hilbert spectral information entropy, and analyzed coal gangue vibration signals based on Hilbert-Huang transform [22]–[24]. Xue *et al.* extract the vibration signals of the tail beam of the hydraulic support under different conditions of caving coal, caving gangue and caving roof with a portable vibration data recorder developed by themselves, and put forward the coal-rock recognition method based on the energy analysis to wavelet packet frequency bands [25]. Hobson *et al.* established a set of coal gangue separation process based on image processing and analysis, and found that texture is more suitable for the application of coal gangue separation [26]. Mu *et al.* put forward a coal gangue detection method based on the cooperation of FPGA and DSP [27]. Xu *et al.* proposed a coal-rock interface recognition method based on Mel-Frequencyepstrum coefficients and neural network, separate acoustic signals by using Independent Component Analysis (ICA), and used the BP neural network to recognize coal-rock interface after extracting MFCC features [28]. Wang *et al.* combined the improved particle swarm optimization algorithm with the wavelet neural network to identify the change of cutting load of the shearer, which provide a scheme for the cutting state identification [29]. Si *et al.* proposed an intelligent multi-sensor data fusion recognition method based on parallel quasi-Newton neural network (PQN-NN) and Dempster-shafer (DS) theory to recognize the cutting state of shearers [30]. Wang *et al.* carried out the study on the vibration state of tail beam and the identification of coal gangue interface in top coal caving process based on time series analysis, Hilbert marginal spectrum distribution characteristics, EMD and neural network [31]–[33]. Hua *et al.* took the vibration signal of tail beam as the research object and proposed a method for interface recognition of fully-mechanized caving face based on dimensionless parameters and SVM [34]. Zhang *et al.* analyzed the vibration acoustic signal of coal and gangue by Hilbert-Huang transform, and obtained the frequency and amplitude characteristics of the acoustic signal under the conditions of top coal falling and coal gangue mixture [35]. Li proposed an effective edge detection algorithm to extract edges from coal gangue noise images, which improved the recognition rate of gangue [36]. Song *et al.* designed an automatic control system for caving process in top coal caving mining, proposed a new multi-class feature selection approach based on vibration and acoustic signal, and an effective minimum enclosing ball (MEB) algorithm plus SVM is proposed for rapid detection of coal-rock in the caving process [37]–[39]. Based on image analysis and Relief-SVM Dou *et al.* identified coal and gangue under four different working conditions [40]. Li *et al.* studied the recognition of coal and gangue through the image processing [41]. Based on extensions of the co-occurrence matrix method and Multispectral and Joint Color-Texture Features, Tripathy *et al.* identified the associated gangue minerals from limestone and coal mines using three different approaches [42]. Zhang *et al.* proposed to detect the instantaneous refuse content of drawn coal and gangue mixture during top coal caving by using natural gamma-ray technology, and conduct experiments to identify the mixed condition of roof-rock by using the self-developed coal-gangue recognition experimental system [43]. Based on

partial gray compression and extended-order co-occurrence matrix, Yu *et al.* proposed an image recognition approach for coal and gangue [44]. The above research provides a foundation and reference for coal rock recognition in top coal caving. However, due to the complex working conditions underground, more dust, noise, different distribution of coal seams, and the existence of particle disturbance and other conditions, there is still a big gap between the various methods and the actual application of the coal gangue identification in the top coal caving, and the identification approach is not perfect.

According to the previous research achievements on the spherical contact and the spherical plate contact [45]–[60], and after the collision and slippage behavior analyze between the coal gangue and the metal plate of the hydraulic support in the process of top coal caving, we have studied the systematic dynamic and contact response for the rock sphere elastic impact on the metal plate and for the coal gangue-like elastic spherical particle impact on the elastic half-space [61], [62], and preliminarily proved the exist of the difference between the contact responses and the vibration signals when coal gangue impact on the metal plate respectively, which explains the identifiability of coal and gangue. Based on the above research, and in order to finally break through the problem of the coal gangue surface identification in the top coal mining, we innovatively put forward to disassemble the complex coal gangue recognition problem in top-coal caving, adopt the approach of breaking up the whole into parts and research from point to face, and took the single particle coal gangue recognition as a breakthrough point, through constructing the vibration testbed of single particle impacting metal plate and conducting large sample single particle coal gangue impact test, combined with signal acquisition, signal interception, Hilbert-Huang transform and other processing methods, as well as machine learning and deep learning and other classification methods, the identification of the single particle coal gangue based on the impact vibration signal of metal plate is completed finally, and the recognition scheme is discussed considering the different recognition sample data and the specific application requirements.

The remainder of the paper is organized as follows: Section 2 designs and introduces the single particle coal gangue impact testing system and the experimental scheme. Section 3 introduces the standardized processing method of the signal intercepted. Section 4 extracts the signal traditional time domain characteristics and time-frequency characteristics and determines the 10 recognition features. Section 5 conducts the recognition of single coal gangue based on the recognition Eigenvector. Section 6 conducts the recognition of single coal gangue based on the original intercepted signal, and discusses the selection basis of recognition scheme. Section 7 shows some related work and our conclusions.

II. EXPERIMENT DESIGN

Collision contact and relative sliding friction between the coal gangue and the tail beam cause the vibration response of the tail beam. However, in the process of top coal caving, underground condition is complicated and the number of coal gangue particles is large, there are complex particle interaction and collision behaviors between coal gangue and the metal plate of the tail beam and shield beam. This greatly increases the difficulty of the research on the recognition technology of coal gangue under the cover of all factors, which leads to the inability to clearly understand the essential causes of signal generation and the real propagation law under various field conditions. It seriously restricts the theoretical development of coal gangue recognition based on data analysis and the practical application of coal gangue recognition technology in top coal caving mining. Therefore, this paper adopts the research method of breaking up the whole into parts, only based on the study of single particle coal gangue direct impact on the metal plate, and carries out the research on the identification technology of coal and gangue based on single particle coal gangue direct impact on the metal plate through single particle impact vibration test in the laboratory and impact vibration response analysis. The design and test scheme of the single particle impact test system is described as follows:

A. DESIGN OF THE IMPACT TEST SYSTEM

In this paper, single particle coal gangue impact on the metal plate is taken as the direct research object. Single particle impact test system mainly realizes the functions of vertical impact between coal gangue and the metal plate, the extraction of vibration signal as well as the subsequent signal processing. According to this, single particle impact test system is constituted by the impact object (coal gangue), impact test-bed, signal acquisition system and signal analysis system four parts, as is shown in Figure 2.

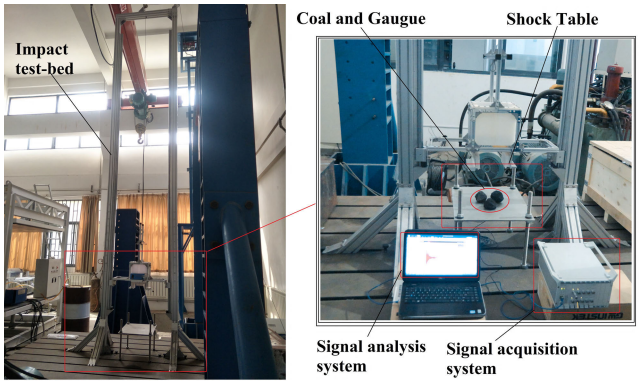

FIGURE 2. Single particle impact test system.

Among them, the impact test-bed is responsible for discharging coal gangue and completing particle impact on metal plate test. The structure of the impact experiment table is shown in Figure 3.

As is shown in the figure, the impact test-bed is mainly composed of supporting portal frame 1 (European standard 8080Q aluminum alloy profile), cylindrical guide rail 2, steel

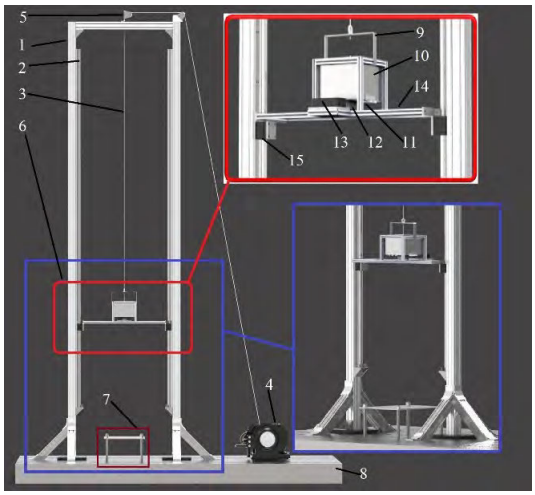

FIGURE 3. Single particle impact test-bed.

wire rope 3, winch 4, lifting pulley 5, moving coal dropping device 6, shock table 7 and T-shaped platform 8. Supporting portal frame is fixed on the T-shaped platform to support the cylindrical guide rail and the moving coal dropping device, and the cylindrical guide rail is installed on the inner side of the supporting portal frame. The shock table is composed of the screw rod, the fixing nut and a metal plate, which is fixed on the T-shaped platform through the T-shaped slider and the screw rod, and the metal plate is fixed on the screw rod through the fixing nut on the upper and lower sides. The moving coal dropping device is composed of lifting cross rod 9, blanking port 10, valve 11, electromagnetic lock 12, electromagnetic lock controller 13, moving frame 14 and slider 15. The lifting cross rod is fixed on the upper end of the blanking port and connected with the steel wire rope, two rotational valves installed on the bottom of the blanking port, the blanking port and electromagnetic locks as well as the electromagnetic lock controller are fixed in the moving frame. Two rotational valves can be opened and closed under the action of electromagnetic locks and the electromagnetic lock controller. The moving frame is fixedly connected with the slider so as to realize the integral sliding connection of the moving coal dropping device on the cylindrical guide rails on both sides, and then the moving coal falling device can vertical lifting go up and down along the cylindrical guide rail under the action of the comprehensive action of the winch, the lifting pulley and the steel wire rope. The center point of the metal plate of the shock table and the center point of the moving coal dropping device are located on the same vertical line.

The main function of the signal acquisition system is to realize the acquisition and storage of the original test data. It mainly includes signal detection device sensor and acquisition device. This paper mainly studies the vibration signal of metal plate after it is impacted by single particle coal and gangue, so the test data to be collected is the vibration signal of metal plate. In order to accurately obtain the

FIGURE 4. Sensor 1A102E.

vibration signal of the metal plate, the general piezoelectric acceleration sensor 1A102E of DongHua testing company was selected. The sensor is shown in Figure 4. It has a wide measuring range, a small strain on the base, a shear design and a minimum output impedance, which are not easily affected by external factors. Its mass is only 5.6g, and it has little interference to the vibration attenuation of the vibration metal plate. The sensor is equipped with a magnet at the end, which can be directly mounted on the metal plate for magnetic adsorption, it is convenient and fast, and is very suitable for quick and effective acquisition of vibration signals at the top coal caving condition, and can reduce disturbance factors during signal acquisition.

TABLE 1. Parameters of the sensor 1A102E.

Type	1A102E
Sensitivity(mV/g)	10
Measuring range (g)	±500
Frequency (Hz±10%)	0.5~10,000
Resolution ratio ($m \cdot s^{-2}$)	0.005
Impact limit (g)	5,000
Temperature (°C)	-40~+120
Boundary dimension (mm)	ϕ10×22
Weight (g)	5.6
Install type	M5
Output	Top L5
Form	Single-track

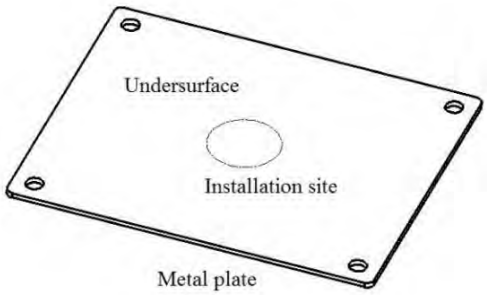

FIGURE 5. Installation of the sensor.

The specific parameters of the sensor are shown in Table 1. In order to improve the effectiveness of the collected signals, the acceleration sensor is installed in the central position of the bottom of the metal plate, as is shown in Figure 5.

FIGURE 6. DH8302 dynamic signal acquisition system.

The acquisition device is DH8302 dynamic signal acquisition system, as showed in Figure 6. This system has the advantage of high bridge pressure automatic calibration, and can timely capture the real-time status of different channels through the field calibrated stress and strain channels. The measurement parameters can be set automatically according to the requirements of the project and the set module, and it also has the function of intelligent wire identification. Real-time and effective transmission of data is realized through DMA, which ensures that the collected data is high-speed, not dead, effective, stable and not leaking during the transmission process. It communicates with the computer through the GbE gigabit Ethernet, so that the communication between different channels can be achieved continuous real-time, multi-channel signal measurement and storage records, and the parallel work can be completed synchronously between the channels. The channel is flexible and easy to operate, it can test and analyze various physical quantities such as force, electricity, impact, acoustics and voltage, etc. By selecting and matching charge adapter and piezoelectric sensor, the dynamic pressure and acceleration can be accurately collected. And it has the extremely high test precision and the anti-interference ability, which guarantees the accuracy of the collection results. Therefore, the DH8302 high-performance dynamic signal acquisition system was selected for signal acquisition.

The analysis system is DHDAS dynamic signal acquisition and analysis system (Figure 7), which can realize the control of DH8302 dynamic signal acquisition system and complete the system setting in the process of signal acquisition, display the collected signals, add basic filtering and other signal preprocessing functions, and save the original signal and pre-processed signal record on PC.

B. TEST SCHEME

In the process of top-coal caving, there are a large number of coal gangue particles with different shapes and sizes, and the impact speed when colliding with the hydraulic support is also different. In order to obtain the test data of coal gangue with different shapes and impacts at different speed, coal gangue with different sizes and shapes are randomly selected and piled up for the test. In the process of caving, the impact velocity of coal gangue and metal plate is different, so the random dropping of coal gangue is adopted in this paper, that is, the height of the randomly selected coal gangue particles is not specified and unified, and the coal gangue is carried out at a certain height through winch, steel wire rope, lifting pulley and moving coal dropping device.

Before the test, parameters of DH8302 dynamic signal acquisition system shall be set and signal pre-processing module shall be added in the DHDAS dynamic signal analysis system in advance. In this paper, single channel is adopted for signal acquisition, sampling frequency is set as 5,000 Hz, and storage mode is continuous storage. The measurement is voltage measurement, the measurement is acceleration of the metal plate when coal and gangue impact, the measurement range is 5,000 m/s, the sensitivity is set as 1, and the input mode is IEPE piezoelectric input. At the same time, the noise reduction module and the anti - mixing filter are turned on to realize the preliminary filtering of the signal. The specific test process is as follows:

(1) Install the sensor at the specified location, open the DH8302 dynamic signal acquisition system and DHDAS dynamic signal analysis system, and complete the parameter setting. Before each impact tests, clear the natural vibration signal of the metal plate. Control the electromagnetic lock of the two valves to close, put the single coal gangue into the blanking port. Then start the winch and bring the blanking device reach to any height along the guide rail through the steel wire rope traction.
(2) Opened the electromagnetic lock remotely by the electromagnetic locking controller, and the coal or gangue free falling and finally impact on the metal plate.
(3) After the metal plate of the shock table is excited by the rock, the vibration sensor and the DH8302 dynamic signal acquisition system collect the acceleration time history response of the vibration metal plate, and transmit it to the DHDAS dynamic signal analysis system in PC to save the data.

Carried out 1,000 groups of coal impact tests first, and labeled as 1-1,000 group of coal impact tests respectively according to the test sequence. After that, 1,000 groups of gangue impact tests are conducted and are labeled as 1-1,000 group gangue impact tests respectively according to the test sequence. The data were classified and saved and 2,000 groups acceleration response data of coal gangue impact on the metal plates are obtained. Caving height of coal and gangue in each impact test is arbitrarily set, and the accurate caving height is not counted.

III. INTERCEPT A PART OF VIBRATION SIGNAL (SIGNAL INTERCEPTED)

After the test is completed, acceleration data after pretreatment exported by the DHDAS dynamic signal analysis system are shown in Figure 8 (Take 3 groups of coal and gangue test data as examples, respectively). According to the figure,

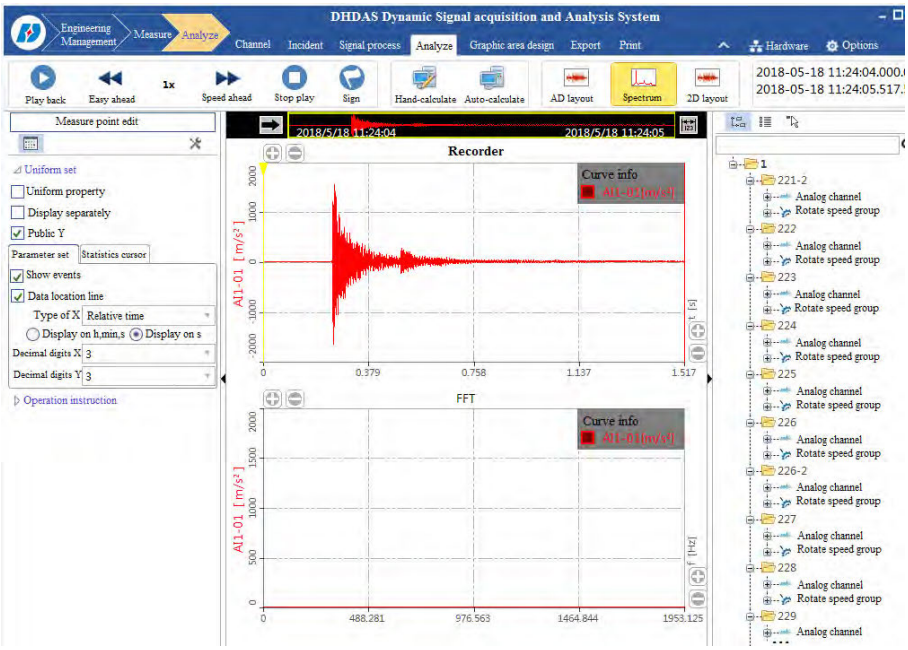

FIGURE 7. DHDAS dynamic signal analysis system.

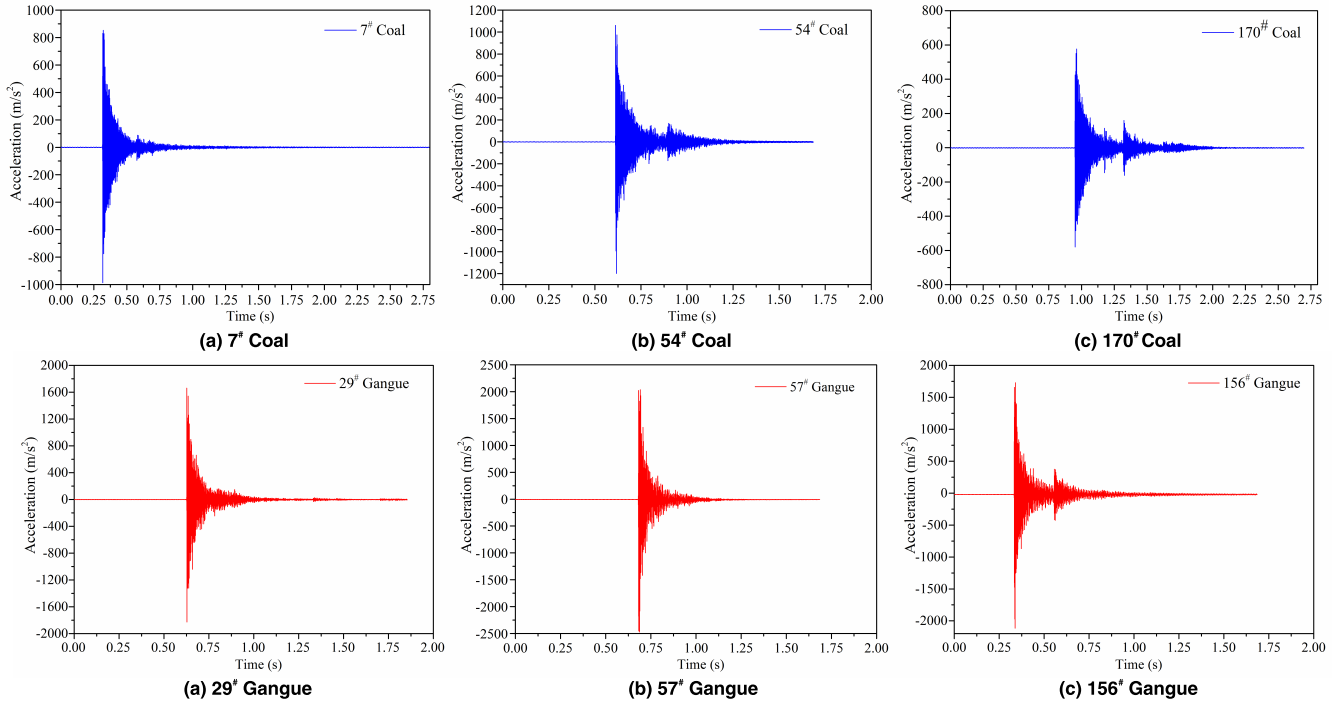

FIGURE 8. Pre-processed acceleration data.

the obtained data are the acceleration records of the metal plate in the whole dynamic process, including the natural vibration of the metal plate before the contact between the rock and the metal plate, and the repeated or multiple collision course after the first collision.

Due to the different falling height of the coal and gangue, the interval time from the falling of coal and gangue to the contact between coal gangue and the metal plate is different. The impact contact speed, the shape and size of coal gangue particles are different, so the re-collision phenomenon after

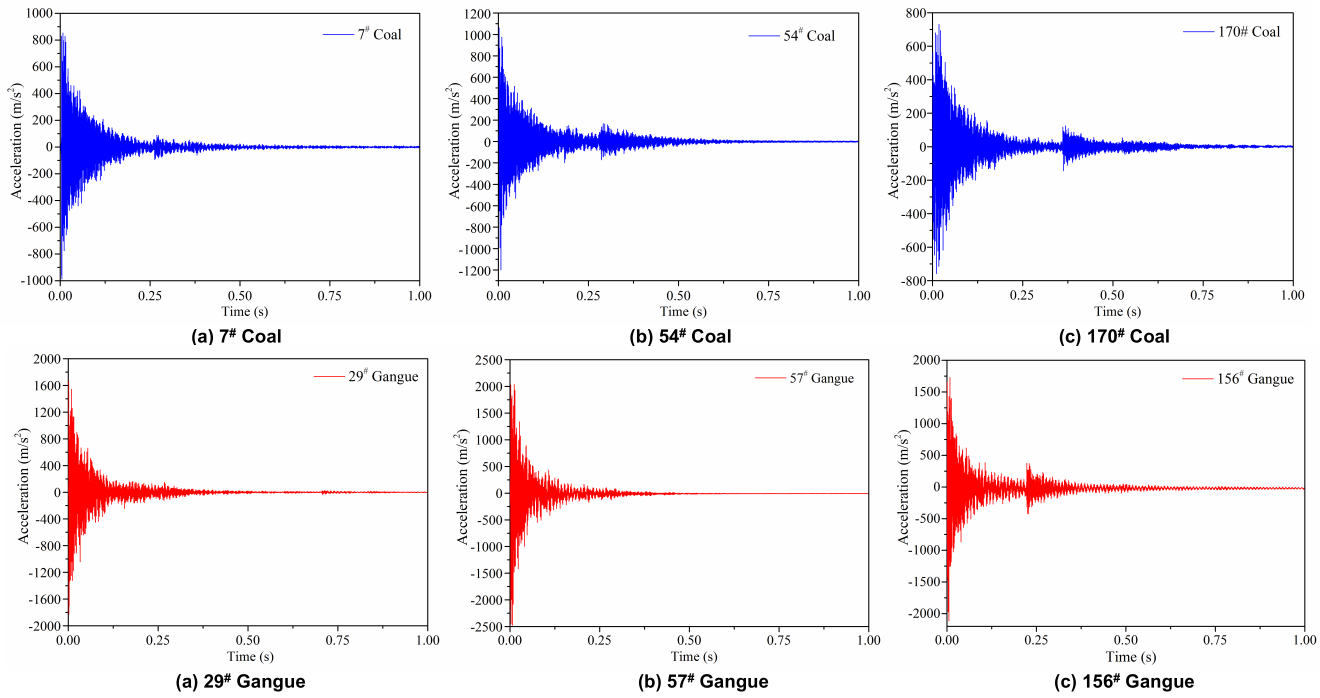

FIGURE 9. Acceleration data after Signal intercepted processing.

the first collision is also different, and the time length of each group acceleration is different. In order to standardize the analysis and facilitate the subsequent signal reprocessing, the 2,000 groups acceleration after pretreatment obtained from the experiments was standardized by means of Signal intercepted, the specific operation is described below: It is observed that the natural vibration acceleration of the metal plate is very small, almost to zero, while the vibration acceleration of the metal plate increases sharply after being impacted (After 3-5 sample points, it can be increased to more than 100 m/s^2.). In this paper, the threshold of data extraction is set at 10 m/s^2, that is to say, the data is valid from the first point greater than 10 m/s^2, and all the 4,999 sample points thereafter are valid data, totaling 5,000 sample points are taken as a set of valid data samples, and the duration of each set of valid data is 1s. The acceleration signal after Signal intercepted is shown in Figure 9.

IV. EXTRACTION OF SIGNAL FEATURES AND DETER-MINATION OF RECOGNITION FEATURES

The vibration signal produced by the impact of coal gangue on the metal plate is non-stationary and nonlinear, which cannot be expressed by accurate time function relation, but can only be described by mathematical methods of probability and statistics. In order to identify coal and gangue according to the difference of impact vibration signals, signals are processed in this paper. Through a certain mathematical theory and algorithm, extracts characteristic indexes that can effectively reflect the metal plate vibration signals produced by the impact of coal gangue from the non-stationary vibration signals, so as to further identify the signals.

A. EXTRACTION OF THE TRADITIONAL TIME DOMAIN FEATURE

After the Signal intercepted processing, each group vibration signal of the metal plate after coal gangue impact test is quantified into a discrete sample containing 5,000 signal points. The traditional time domain parameters such as the mean value (y_J), the absolute mean value (y_{JJ}), the square root amplitude (y_{FF}), the variance (y_{FC}), the skewness (y_{PX}), the kurtosis index (y_{QD}), the Peak-to-Peak value (y_{F-}), the margin index (y_{YD}), and the waveform index (y_{BX}) of each group vibration signal were calculated respectively. The specific calculation formulas are shown in follows:

$$y_J = \frac{1}{m}\sum_{p=1}^{m} y_p \tag{1}$$

$$y_{JJ} = \frac{1}{m}\sum_{p=1}^{m} |y_p| \tag{2}$$

$$y_{FF} = (\frac{1}{m}\sum_{p=1}^{m}\sqrt{|y_p|})^2 \tag{3}$$

$$y_{FC} = \frac{1}{m}\sum_{p=1}^{m}(y_p - y_J)^2 \tag{4}$$

$$y_{PX} = \frac{1}{m}\sum_{p=1}^{m} y_p^3 \tag{5}$$

$$y_{QD} = \frac{\frac{1}{m}\sum_{p=1}^{m}(y_p - y_J)^4}{y_{FC}^2} \tag{6}$$

$$y_{F-} = y_{p\max} - y_{p\min} \tag{7}$$

TABLE 2. Traditional time domain parameters of the coal.

Serial number	Mean value	Absolute mean value	Square root amplitude	Variance	Skewness	Kurtosis index	Peak-to-Peak value	Margin index	Waveform index
1	-0.145	22.065	486.861	2,123.1	11,610.0	27.246	971.35	1.072	2.088
2	-0.166	45.001	2,025.100	16,235.0	-561,600.0	34.637	2,647.70	0.630	2.832
3	-0.374	28.258	798.501	6,214.8	-591,830.0	48.646	2,161.00	1.059	2.790
4	0.903	41.175	1,695.400	12,922.0	-609,300.0	45.998	3,203.90	0.725	2.761
5	-0.173	33.947	1,152.400	11,076.0	1,320,900.0	83.672	3,449.80	1.209	3.100
6	-0.709	14.387	206.990	635.9	-1,530.8	9.600	346.08	0.918	1.753
7	-0.505	47.123	2,220.500	9,198.1	-333,150.0	29.671	2,104.70	0.429	2.035
8	-0.986	30.587	935.541	4,161.2	2,502.1	20.636	1,156.20	0.616	2.109
9	-1.012	30.929	956.614	3,397.7	35,347.0	15.334	873.19	0.506	1.885
10	-1.164	39.627	1,570.300	10,519.0	163,030.0	25.628	2,131.00	0.729	2.588
11	-1.126	35.575	1,265.600	5,198.4	34,274.0	17.849	1,237.80	0.537	2.027
12	-1.159	31.425	987.534	4,149.0	46,941.0	27.000	1,536.50	0.769	2.050
13	-0.884	60.678	3,681.800	18,669.0	44,691.0	32.144	2,922.10	0.366	2.252
14	1.102	33.809	1,143.100	6,369.4	-28,226.0	26.426	1,487.70	0.639	2.361
15	0.245	30.162	909.742	4,852.3	110,240.0	33.597	1,675.20	0.938	2.310

TABLE 3. Traditional time domain parameters of the gangue.

Serial number	Mean value	Absolute mean value	Square root amplitude	Variance	Skewness	Kurtosis index	Peak-to-Peak value	Margin index	Waveform index
1	-20.749	64.561	4,168.1	21,047.0	-2,443,300	50.283	3,842.6	0.415	2.270
2	-22.021	73.210	5,359.7	43,050.0	-190,240	66.007	5,742.1	0.433	2.850
3	-0.830	45.612	2,080.4	15,949.0	305,990	53.167	3,694.9	0.885	2.769
4	5.732	61.132	3,737.2	27,244.0	-1,089,600	49.240	4,852.3	0.589	2.702
5	31.481	70.409	4,957.4	25,908.0	-3,981,300	58.772	4,378.5	0.447	2.329
6	6.412	54.827	3,006.0	25,840.0	-1,830,600	71.844	5,029.3	0.883	2.934
7	18.063	47.833	2,288.0	11,300.0	-812,070	47.651	2,895.5	0.590	2.254
8	-1.221	53.507	2,863.0	22,196.0	-52,867	63.346	4,380.4	0.835	2.785
9	20.903	67.786	4,595.0	29,683.0	-8,163,300	78.770	5,022.1	0.491	2.560
10	12.090	103.646	10,742.0	67,859.0	4,850,300	46.272	6,627.3	0.345	2.516
11	-27.818	75.067	5,635.0	30,349.0	3,454,200	48.859	4,096.1	0.435	2.350
12	8.127	66.947	4,481.8	31,904.0	-3,498,900	80.975	5,893.6	0.652	2.671
13	21.326	92.486	8,553.7	64,514.0	-8,056,400	50.661	6,614.6	0.391	2.756
14	3.968	74.528	5,554.5	37,027.0	-2,396,100	46.030	4,992	0.447	2.582
15	6.941	66.630	4,439.6	31,502.0	824,890	48.071	4,516.4	0.495	2.666

$$y_{YD} = \frac{y_{p\max}}{y_{FF}} \tag{8}$$

$$y_{BX} = \frac{1}{m}\frac{\sum_{p=1}^{m} y_p^2}{y_{JJ}} \tag{9}$$

where p is the p^{th} sample point of a vibration signal, y_p is the vibration acceleration value of the p^{th} sample point of an intercepted vibration signal, m is the total number of the sample points of each intercepted vibration signal, in this paper m = 5,000, y_{pmax} is the maximum vibration acceleration value of an intercepted vibration signal, and y_{pmin} is the minimum vibration acceleration value of an intercepted vibration signal.

According to the formula, 2,000 sets of test vibration signals are calculated, and 9 traditional time domain parameters of each set of signal are obtained. 15 groups of coal gangue are randomly selected as examples here. The obtained time domain parameters are shown in Table 2 and Table 3.

Comparing the data in the two tables, we can see that: the variance of the vibration signals under coal impact is within the range of [635.9, 18,669], among which only two groups have a variance greater than 15,000. However, the variance of the vibration signal during gangue impact is within the range of [11,300, 67,859]. And only two groups had a variance less than 18669, only one group had a variance less than 15,000, and the other 13 groups vibration signals of gangue impact had variance over 21,000. The vibration signal variance of the metal plate under the impact of gangue is much higher than that of coal.

The Peak-to-Peak value of the metal plate vibration signal during coal impact is within the range of [346.08, 3,449.80], only three of the 15 groups of coal impact vibration signals are higher than 2895. However, the peak-to-peak value of the vibration signal during gangue impact is within the range of [2,895.5, 6,627.3]. Only one group of the peak-to-peak value is less than 3,449.80 while the other 14 groups of gangue impact vibration signals are all above 3,690, and the maximum peak-to-peak value is even more than 6,600. The peak-to-peak value of vibration signals of the metal plate under the impact of gangue is much higher than that of coal.

The kurtosis index of the metal plate vibration signal during coal impact is within the range of [9.600, 83.672], only two of the 15 groups of vibration signals are higher than 47, and the other 13 groups are lower than 46. However, the kurtosis index of the vibration signal during gangue impact is within the range of [46.030, 80.975]. Only two groups of gangue impact vibration signals are lower than 47, and 12 groups are above 48. The kurtosis index of the metal plate vibration signals under the impact of gangue is much higher than that of coal.

The mean value of the vibration signal during coal impact is within the range of [-1.2, 0], while that during gangue impact is within the range of [-27.818, 31.481]. The mean value of the vibration signal under coal impact is within the mean value range of the vibration signal under gangue impact. Although there is a significant difference in the vibration signal mean value of coal gangue impact, it is not suitable for the classification basis of coal gangue signals due to the complete overlap of intervals. The absolute mean value and square root amplitude of the metal plate vibration signal under coal gangue impact have great difference and little overlap of value range. However, five groups of time domain parameters, namely mean value, absolute mean value, square root amplitude, variance and peak-peak value, are belonging to the same type of time domain index, and have the high correlation with each other. All of them are taken as characteristic parameters have little effect on improving the recognition rate.

The skewness of the vibration signal during coal impact is within the range of [-609,300, 1,320,900], while that during gangue impact is within the range of [-8,056,400, 4,850,300]. The skewness of vibration signal under coal impact is within the skewness range of vibration signal under gangue impact and cannot be taken as the identification feature. The margin index of vibration signal during coal impact is within the range of [0.366, 1.209], while that during gangue impact is within the range of [0.345, 0.885], the interval overlap is too high to be used as a recognition feature. The waveform index of the vibration signal during coal impact is within the range of [1.753, 3.100], while that during gangue impact is within the range of [2.254, 2.934], it also can't be taken as the recognition feature.

The signal variance represents the deviation degree between the signal value and the signal center value, which is used to measure the fluctuation of the signal. The peak-to-peak value of a signal refers to the difference between the highest and lowest values of a set of signal sample points, which show the magnitude of the variation range of the vibration signal. The kurtosis index refers to the ratio of the fourth-order center distance to the square of the signal variance, which reflects the impact characteristics of the signal. In this paper, variance, peak-to-peak value and kurtosis index are selected as three identification features from nine traditional time domain parameters.

B. TIME-FREQUENCY FEATURE EXTRACTION BASED ON HHT

HHT [63]–[67] signal processing methods include EMD (empirical mode decomposition) [68]–[76] and HAS (Hilbert spectrum analysis). The IMF component decomposed by EMD can reflect the essential characteristics of signals, and the Hilbert energy spectrum obtained by HAS analysis can clearly show the characteristics of energy distribution at any time and frequency. In order to comprehensively grasp the non-stationary and non-linear vibration signals produced by coal gangue impact on the metal plate and obtain their effective characteristics, this paper uses HHT method to process the signals after standardized intercepted.

1) EMD TO SIGNALS

The vibration signals are decomposed by EMD, and the expression of the Intercepted signals is as follows:

$$y(t) = \sum_{i=1}^{n} c_i(t) + r_n(t) \tag{10}$$

The stopping criterion for decomposition is as follows:

$$S_d(t) = \sum_{t=0}^{T} \frac{\left|h_{q-1}(t) - h_q(t)\right|^2}{h_q^2(t)} \tag{11}$$

Among them, y(t) is the Intercepted signal, $S_d(t)$ is the stop quantization parameter, and it is generally believed that $S_d(t)$ is between 0.2 and 0.3, i is the serial number of the IMF component, ci(t) is the i-th IMF component, $h_{q-1}(t)$ and $h_q(t)$ are sample sequences of the two continuous processing results in the decomposition of the IMF component, q is the q^{th} sample sequence in the decomposition process of the IMF component, $r_n(t)$ is the residual term after n times of EMD, and n is the number of IMF components when decomposition stops, T is the total time length of y(t), t is the time at any sample point.

The vibration signals of metal plates after 2000 groups of coal gangue impact are decomposed by EMD. Take the vibration signals of the metal plate after the impact of the 7^{th} group coal and the 29^{th} group gangue as examples, 10 IMF components and one residual term RES of the signals (That is, after EMD process to the metal plate vibration signal, which is produced by the impact of the displayed coal gangue, $n = 10$) are obtained respectively, as shown in Figures 10-11.

By integrating to the square of the IMF component $c_i(t)$ in time T (T is the total sampling time for each impact signal, $T = 1s$ in this paper), the energy characteristic functions of each IMF component can be obtained:

$$E_i(t) = \int_0^T c_i^2(t)\,dt \tag{12}$$

In Eq. (12), $E_i(t)$ is the energy eigenvalue of the i^{th} IMF component. Through observing the IMF component and its energy value decomposed by EMD of 2,000 groups metal

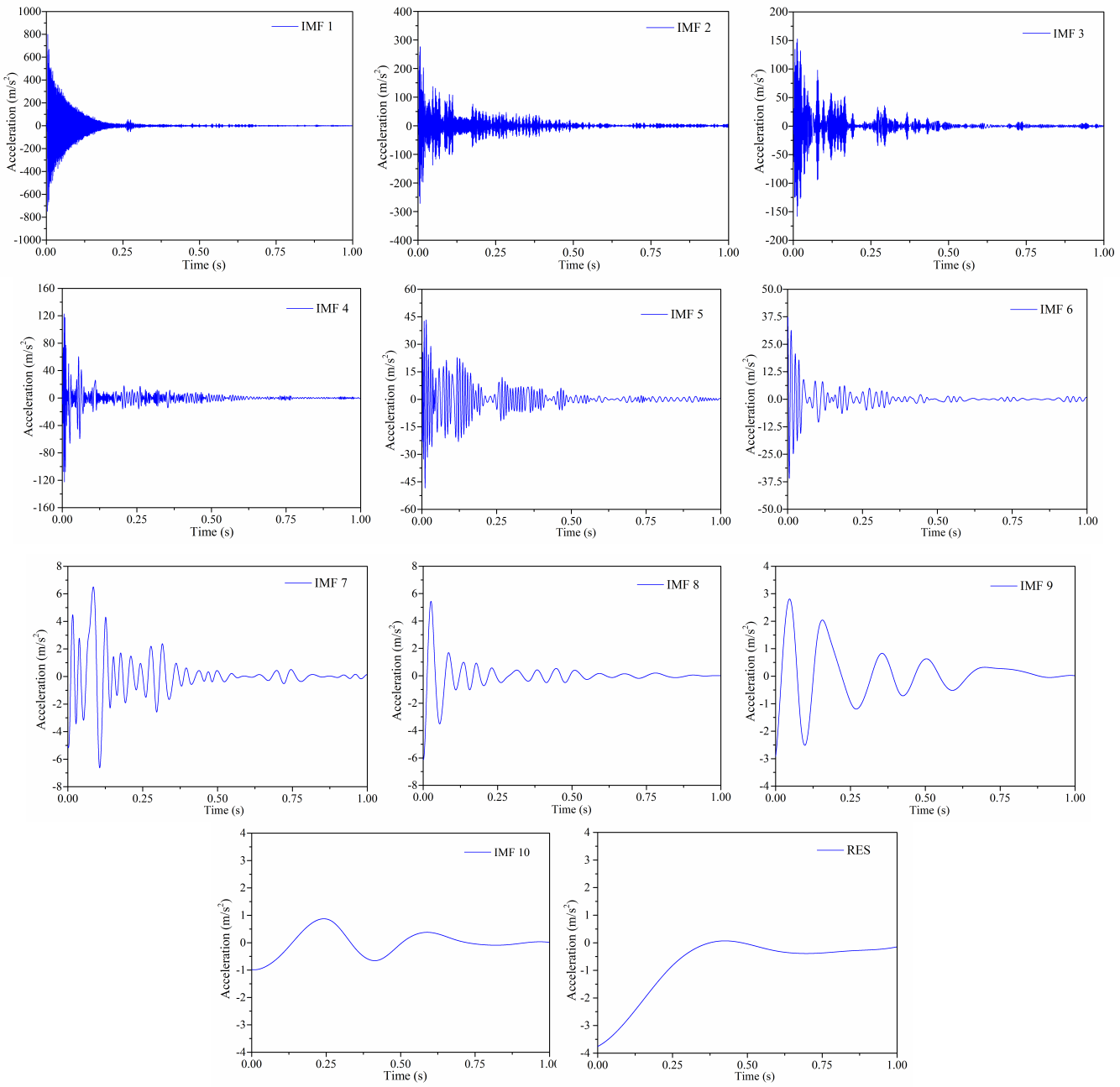

FIGURE 10. EMD process to the vibration signals of the metal plate under coal impact.

plate vibration signals after coal gangue impact, the decay rate of the first 6 IMF components is relatively large and stable, so the energy value of the first six IMF components of each group signal is taken as 6 identification features respectively.

2) HAS TREATMENT OF THE SIGNALS

The $c_i(t)$ of the intercepted vibration signal y(t) decomposed by EMD is transformed by Hilbert transform, and the results are as follows:

$$z_i(t) = \frac{1}{\pi}\int_{-\infty}^{+\infty}\frac{c_i(\tau)}{t-\tau}d\tau \tag{13}$$

After Hilbert transform is applied to each IMF component of the intercepted vibration signal y(t), y(t) can be expressed as:

$$y(t) = \mathrm{Re}\sum_{i=1}^{n}\alpha_i(t)e^{j\beta_i(t)} = \mathrm{Re}\sum_{i=1}^{n}\alpha_i(t)e^{j\int\omega_i(t)dt} \tag{14}$$

where the instantaneous amplitude of the IMF components is $\alpha_i(t) = \sqrt{c_i^2(t) + z_i^2(t)}$, the instantaneous phase is $\beta_i(t) = \arctan\frac{z_i(t)}{c_i(t)}$, the instantaneous frequency is $\omega_i(t) = \frac{d\beta_i(t)}{dt}$, Re means the real part.

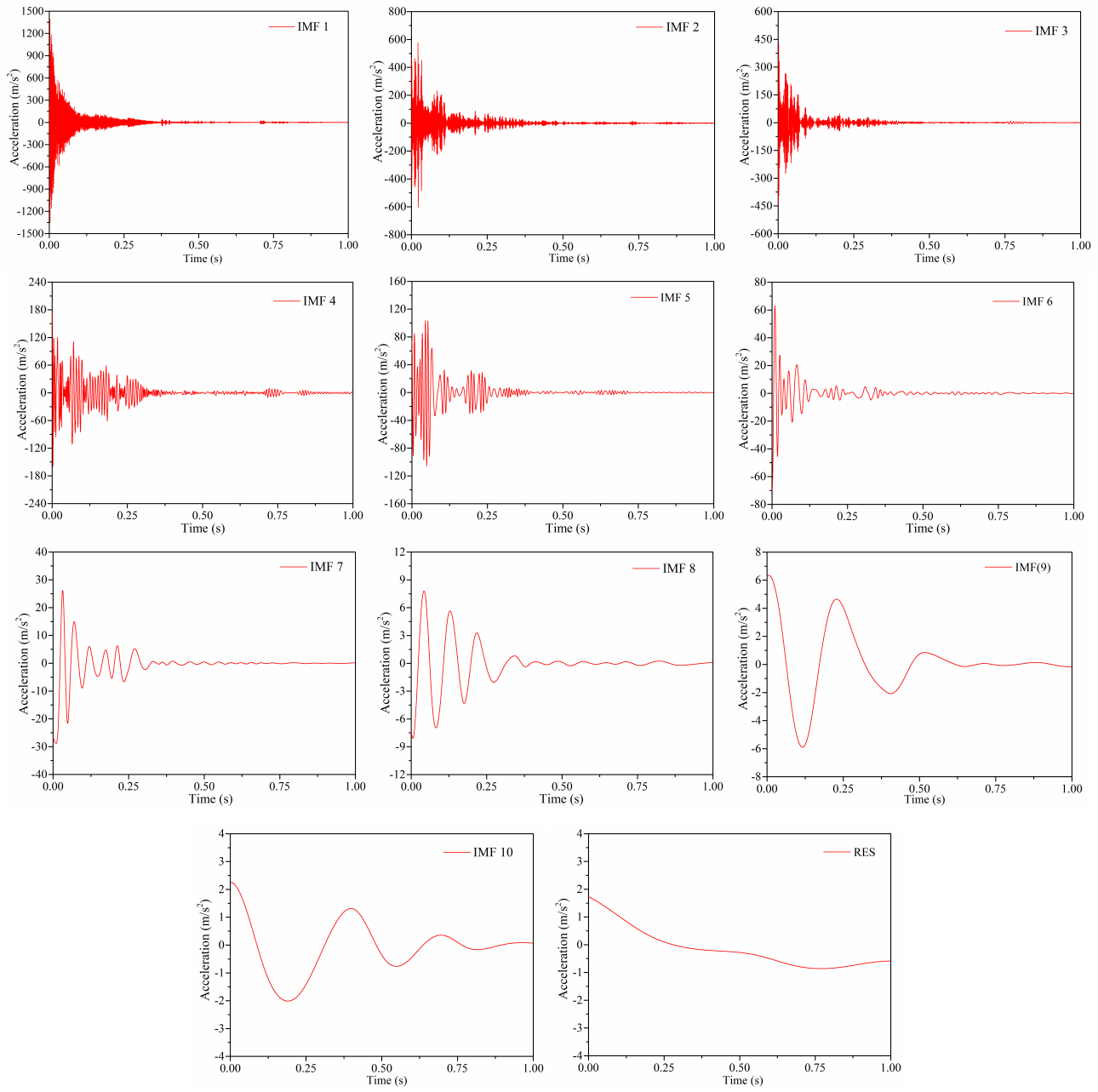

FIGURE 11. EMD process to the vibration signals of the metal plate under gangue impact.

Define ω is the signal frequency, in the above formula, the instantaneous frequency and the instantaneous amplitude of the signal are both functions of time. Based on this, the signal amplitude-time function and signal amplitude-frequency function can be obtained in the form:

$$H(\omega, t) = \begin{cases} \mathrm{Re} \sum_{i=1}^{n} \alpha_i(t)\, e^{j \int \omega_i(t) dt}, & \omega_i(t) = \omega \\ 0, & \text{Other} \end{cases} \quad (15)$$

Taking the vibration signal of the metal plate after the impact of the 7th group coal and the 29th group gangue as the examples, the Hilbert spectrum were obtained after HHT transformation of the signals, as shown in Figure 12:

Integrating the Hilbert spectrum of the signal (Eq. (15)) over time, we can obtain the Hilbert marginal spectrum of the signal h(ω) is:

$$h(\omega) = \int_0^T H(\omega, t)\, dt \quad (16)$$

Hilbert marginal spectrum which reflects the global amplitude or energy contribution of each frequency can accurately represent the amplitude fluctuation of each frequency of impact signal. Taking the vibration signal of metal plate

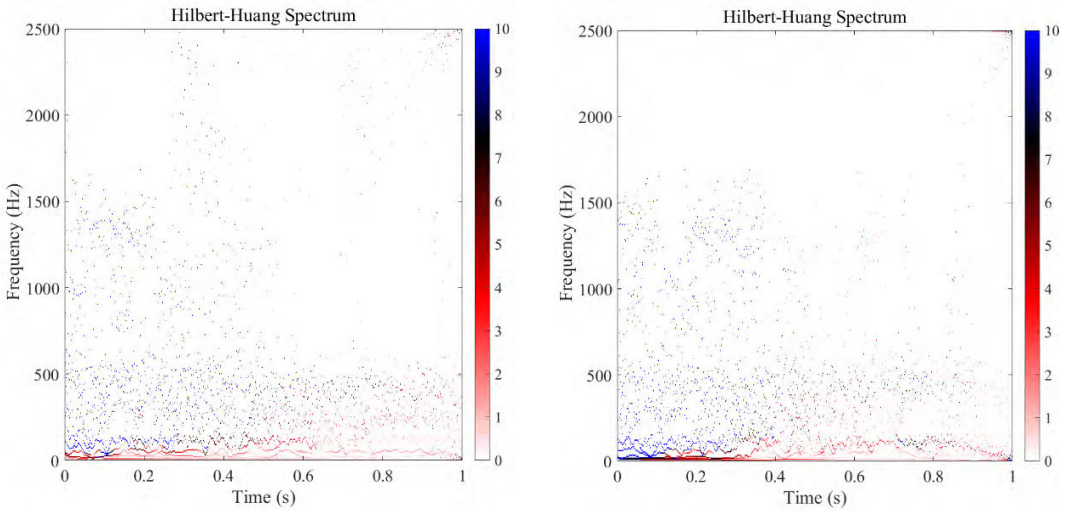

(1) 7th group coal (2) 29th group gangue

FIGURE 12. Hilbert spectrum of the vibration signal when coal gangue impact on the metal plate.

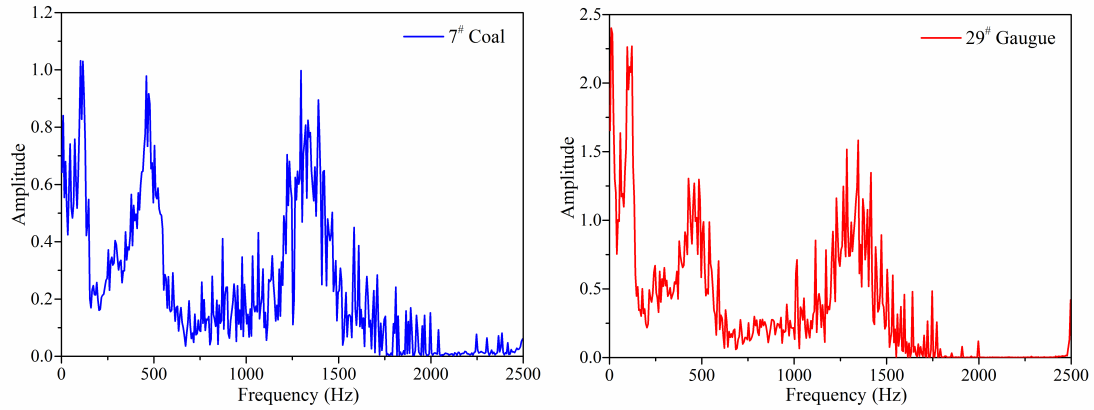

(1) 7th group coal (2) 29th group gangue

FIGURE 13. Hilbert marginal spectrum of the signals when coal gangue impact on the metal plate.

after impact of the 7th group coal and the 29th group gangue as the examples, Hilbert marginal spectrum of the signals were obtained after integrating Hilbert spectrum of the signal, as shown in Figure 13:

By integrating the square of Hilbert marginal spectrum in frequency domain, the energy characteristic functions of the Hilbert marginal spectrum E(ω) are obtained as follows:

$$E(\omega) = \int_{\omega_1}^{\omega_2} h(\omega)^2 \, d\omega \tag{17}$$

where ω_1 and ω_2 are two interval frequencies respectively. In this paper, $\omega_1 = 0$ and $\omega_2 = 2,500$.

According to Eq. (3) and Eq. (8), the vibration signals of metal plates after the impact of coal gangue in Tables 3-4 are processed respectively, and the energy values of the IMF components and the energy of the Hilbert marginal spectrum are obtained, as shown in Tables 4- 5.

According to Tables 4-5, the range of the Hilbert marginal spectral energy value in the 15 groups of coal impact vibration signal is [6.673, 1×10^5, 6.466, 1×10^6]. Only one group Hilbert marginal spectral energy value of the vibration signal was higher than 5.976, 8×10^6 in total 15 groups coal impact, while the rest were lower than 4.1×10^6. The Hilbert marginal spectral energy value range of the vibration signals when gangue impact is [5.976, 8×10^6, 2.077, 5×10^7], only two groups were lower than 6.4661 $\times$ 10^6, and the rest were higher than 8.3×10^6. The Hilbert marginal spectrum energy values of the metal plate vibration signals in gangue impact are significantly higher than that of coal, and the ranges of the Hilbert marginal spectrum energy values when coal gangue impact are less overlapped, so it can be used as a recognition feature.

In the end, this paper determined 10 features, including the variance, peak-to-peak value, kurtosis index, energy value of the first six IMF components and the Hilbert marginal

TABLE 4. Energy of the IMF components and the hilbert marginal spectrum after coal impact.

No.	IMF1 (10^{10})	IMF2 (10^{10})	IMF3 (10^{10})	IMF4 (10^{10})	IMF5 (10^{10})	IMF6 (10^{10})	Hilbert marginal spectrum (10^{7})
1	0.598,1	1.221,0	0.073,5	0.454,8	0.010,8	0.109,7	0.405,98
2	0.045,17	0.092,45	0.342,09	0.016,5	0.070,1	0.010,45	0.111,48
3	0.442,2	0.120,8	0.119,1	0.692,5	0.256,6	0.570,7	0.302,79
4	0.055,9	0.164,53	0.060,5	0.022,1	0.011,0	0.017,5	0.159,39
5	0.261,9	1.068,4	0.005,2	0.019,3	0.003,3	0.574,3	0.253,58
6	3.228,2	0.519,5	0.055,9	0.446,9	0.229,3	0.016,1	0.066,731
7	0.646,4	0.459,04	0.171,4	0.323,0	0.005,9	0.006,6	0.108,84
8	0.028,3	0.004,799	0.003,5	0.004,1	0.025,4	0.057,2	0.069,947
9	0.016,4	0.594,05	0.004,4	0.180,1	0.032,3	0.414,4	0.179,85
10	0.031,2	0.359,2	0.001,6	0.002,7	0.016,1	0.002,3	0.112,98
11	0.067,0	0.607,5	0.001,1	0.125,6	0.038,1	0.009,6	0.101,41
12	0.038,5	0.053,8	0.027,2	0.821,1	0.086,9	0.031,1	0.149,53
13	0.103,6	2.612,9	5.497,0	6.915,5	0.506,3	1.257,5	0.646,61
14	0.924,2	0.013,1	0.161,2	0.994,5	0.004,8	0.034,5	0.247,19
15	0.088,4	0.077,8	0.003,4	0.074,8	0.008,2	0.049,0	0.102,17

TABLE 5. Energy of the IMF components and the hilbert marginal spectrum after gangue impact.

No.	IMF1 (10^{10})	IMF2 (10^{10})	IMF3 (10^{10})	IMF4 (10^{10})	IMF5 (10^{10})	IMF6 (10^{10})	Hilbert marginal spectrum (10^{7})
1	1.041,7	0.699,4	0.228,6	0.882,6	3.627,3	0.042,5	1.005,2
2	0.635,2	2.574,749	0.064,7	0.104,5	0.338,7	0.258,8	0.833,61
3	1.023,6	15.263,0	0.025,9	0.117,1	0.115,8	0.015,9	1.539,5
4	2.718,6	2.911,0	0.494,5	3.567,9	1.903,6	0.812,8	1.381,4
5	6.279,7	0.831,916	0.324,1	2.893,5	0.741,8	0.018,0	1.414,0
6	27.624,3	5.970,9	0.841,1	0.041,3	0.253,6	0.033,7	1.497,6
7	1.484,3	0.187,1	1.133,4	8.376,8	0.513,9	0.607,9	2.077,5
8	2.206,5	0.816,786	1.559,8	0.257,3	8.783,2	0.322,0	0.641,31
9	0.089,1	2.430,7	0.085,6	0.031,2	0.018,7	3.914,6	1.250,8
10	0.228,7	1.333,6	0.609,4	0.209,7	0.579,6	0.907,5	1.009,5
11	0.289,1	0.339,149	0.163,3	1.874,4	0.799,6	0.055,9	0.597,68
12	19.603,2	1.167,0	0.025,0	5.392,3	3.352,4	1.133,9	1.385,2
13	0.374,1	2.085,8	0.496,6	2.489,3	2.494,1	0.456,6	0.878,69
14	0.799,2	2.759,882	2.315,0	0.629,9	1.294,2	2.618,5	0.990,03
15	4.265,6	1.913,5	3.446,0	0.226,0	13.622,7	0.050,2	1.510,4

spectrum energy value, to constitute the feature vector of coal rock detection.

V. RECOGNITION OF SINGLE PARTICLE COAL GANG-UE BASED ON VIBRATION SIGNAL RECOGNITION FEA-TURE VECTOR AND STACKING INTEGRATION

The essence of the single particle coal gangue recognition is to classify the active impact body (coal and gangue) based on the difference of the metal plate vibration signals after coal gangue impact. Based on the feature vector of the vibration signals, the classification algorithm is applied to identify the single particle coal and gangue.

A. SINGLE PARTICLE COAL GANGUE RECOGNITION BASED ON THE VIBRATION SIGNAL RECOGNITION FEATURE VECTOR AND THE GENERAL CLASSIFICA-TION ALGORITHM

In the field of computer, machine learning methods such as Bayesian, Support Vector Machine (SVM), Logic Regression, Decision Tree, and in-depth learning methods based on Neural Network have been proposed for the material recognition and classification. Based on the recognition features extracted from the vibration signals obtained by the experiments, this paper selects 6 kinds of machine learning and in-depth learning algorithms include Decision Tree (DT) algorithms [77]–[81], Random Forest (RF) algorithm [82]–[86] based on bagging algorithm, XGBoost algorithm [87]–[90] based on boosting algorithm, Long short-term memory neural network (LSTM) [91]–[95], Support vector machine (SVM) algorithm [96]–[101] based on minimum risk principle and Factorization Machine algorithm (FM) [102]–[105] for coal gangue detection. In 2,000 groups of coal gangue impact test, 1,600 groups of data (800 groups of the coal and 800 groups of the gangue) were selected for model training, and the remaining 400 groups of data were used for model accuracy testing.

1) ARITHMETIC PARAMETER SETTING

The algorithms used in this paper are all those in sklearn model library called from the Jupyter Notebook program of the Anaconda 3 GPU software. Parameters of each algorithm are set as follows:

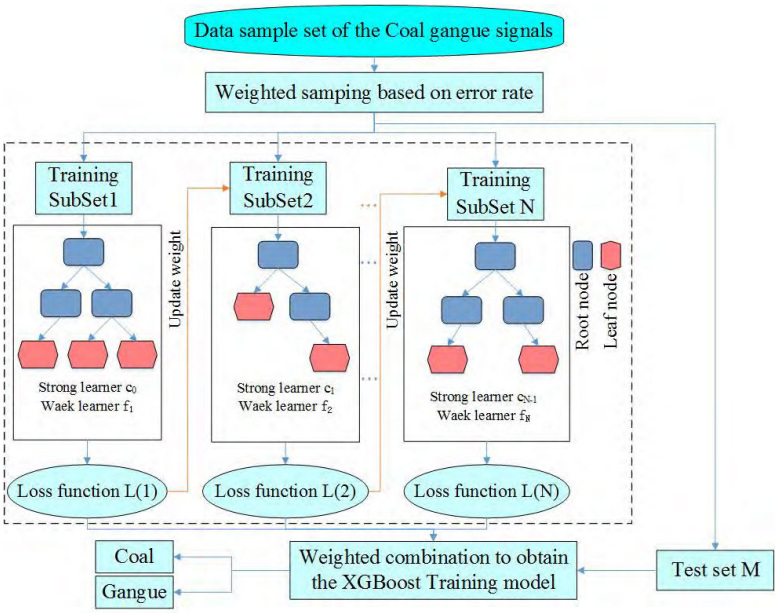

FIGURE 14. The flow chart of the coal gangue impact signal recognition by XGBoost.

1) *XGBoost:* The classifier function is selected as XGB-Classifier. Parameters type includes three kinds: routine parameters, model parameters and learning task parameters. And for the routine parameters, acquiescent Gbtree regression tree model is selected for the booster. Only the final result is needed, and there is no need to output the intermediate process, so here silent is set to 0. To speed up the computation, all CPUs are used for parallel computation, so the nthread is set to −1. More subtrees can make the model have better performance, but too many subtrees are easy to cause over-fitting, based on this, for the model parameters, n_estimatores is set to 300. The depth of the tree affects the fitting effect, the larger the value is, the easier it is to over-fit; the smaller the value is, the easier it is to under-fit. Its typical value is 3-10, here max_depth is set to 5. In this paper, there are 2000 groups test data, 1600 groups are taken as the training set and 400 groups as the test set, so the subsample is set to 0.8. Min_child_weight and colsample_bytree are defaulted to 1. For the learning task parameters, gamma is default to 0 and lambda is set to 1. The output recognition rate is required, so the objective chooses the logistic probability function. learning_rate is set to 0.5. The flow chart of the coal gangue impact signals recognition by XGBoost is shown in Figure 14.
2) *RF:* The classifier function is selected as RandomForestClassifier. The Framework parameters include n_estimators, oob_score and criterion three kinds. For the n_estimators, adopt the maximum number is 100, oob_score is set for True. Criterion is correspondence to the CART classification tree, and take the Gini index as the evaluation standard. The decision tree parameters in the random forest are set as follows: max_feature is set to "auto", max_depth is set to "default", min_samples_split is set to 2, min_samples_leaf is set to 1, min_weight_fraction_leaf is default to 0, max_leaf_nodes is default to "None", bootstrap is set to "True".
3) *LSTM:* input_dim is set as 4000, output_dim is set as 64, activation ="sigmoid", loss is set as "binary_crossentropy", optimizer is set as "rmsprop", metrics is set as "accuracy", batch_size =100, epochs = 5.
4) *DT:* random max_depth is set to 10, decision_function_shape is ovr; criterion correspondence to the CART classification tree, splitter is set to "best", max_features is set to "auto", min_samples_leaf is set to 1, and min_samples_split is set to 2.
5) *SVM:* SVM adopt the sklearn.svm.SVC(), the penalty coefficient c of the error term is default to 1, kernel use the linear kernel function, gamma is set to auto, probability is set to True, decision_function_shape is set to ovr, Probability is set to "False", and cache_size is set to "200".
6) *FM:* Task is set as "classification", num_iter is set to 5, and loss adopt the sigmoid function.

The rest non-setting parameters of the study all are adopting the system default setting. The parameters shown above in the research have already been adjusted to achieve the optimal recognition results of the each model as far as possible. The parameter adjusting process is tedious, and some parameters have little influence on the final results before and after the parameter adjusting. Meanwhile, the parameter adjusting is

TABLE 6. Recognition success rate of the six selected algorithms (%).

Train no.	DT	RF	XGBoost	LSTM	SVM	FM
1	85.75	91.25	92.25	83.92	88.5	51.75
2	86.75	89	91	83.98	91.5	50.5
3	85.5	91.5	91.75	84.61	89.5	48.75
4	85.25	92	90.75	84.86	90.25	44
5	85.5	89.75	91.25	85.04	89.75	50
6	87.75	90.5	90	83.85	91	48.25
7	86	91.75	89.5	85.29	90.5	37.75
8	87.75	90.25	91	84.67	90.5	69
9	87.25	90	90.5	84.42	91.25	62.25
Average recognition rate	86.39	90.67	90.89	84.52	90.31	51.36
Average time(s)	0.221	0.855	0.689	1.745	0.294	0.089

not the focus in this paper, therefore this process is not show in the article.

2) RECOGNITION BY THE GENERAL CLASSIFICATION ALGORITHM

In order to prevent the error of recognition accuracy and response time caused by the contingency of single group experiment, 9 times training and 9 times corresponding test experiments were carried out for the six selected algorithms, and the recognition success rate of the 400 groups of coal gangue test data is obtained, as shown in Table 6.

From Table 6, it can be seen that from training to the recognition completed, the computing time of the six algorithms is within 2s, and the response speed is faster. If the training model is generated in advance, the speed of the coal gangue recognition will be greatly improved. Based on this, it can be inferred that the time just for the single coal gangue identifying stage is very short, and the calculation time of the several models can meet the application requirements. The average recognition rates of random forest, XGBoost and SVM algorithms are above 90%. The average recognition rate of the other three models is lower than 86.5%, and the recognition effect of the other three models is poor. Therefore, the recognition success rate of random forest, XGBoost and SVM algorithm in the 6 selected models is higher. However, the average recognition rate of the six algorithms is less than 91%, and the recognition rate needs to be further improved.

B. DETERMINE THE OPTIMAL IDENTIFICATION SCHEME BASED ON STACKING INTEGRATION

Stacking algorithm [106]–[112] is an ensemble learning algorithm that can combine multiple different categories classification algorithms. Based on the same data samples, different basic classifier models are trained by different classes of algorithms. Then the output data of these classifiers are input into the meta classifiers as the meta-features, and a new classifier model is trained as the final classification from the meta classifiers. The Stacking model can effectively improve the classification accuracy. Using Stacking algorithm, the Random forest, XGBoost and SVM, which have the high recognition success rate, were selected as the recognition base model, and the meta classifier was trained by fusing the three above algorithms with Logistic regression function to develop a new single particle coal gangue fusion recognition model. The single particle coal gangue recognition process based on Staking integration is shown in Figure 15.

The detailed recognition scheme is as the follow:

(1) N groups (In this paper, N is 1600, 800 groups coal and 800 groups gangue) of 2000 groups coal gangue vibration signal samples (1000 groups coal and 1000 groups gangue) were taken as the training set, and the rest M groups (In this paper, it is the rest 400 groups) as the test set. Random Forest, XGBoost and SVM algorithms were used as the base classifier, and take the training subset 1, training subset 2...the training subset N is the verification set in turn, and N-1 parts subsets are the training set. N-fold cross-validation training is conducted to obtain the base trainer, and the recognition and the prediction are made on the respective test sets. In the Random Forest algorithm model, N training predicted values and test predicted values are obtained, and N predicted values of the training set are superposed to get X1, and N predicted values of the training set are averaged to get Y1, and the XGBoost (X2,Y2) and SVM (X3,Y3) algorithm models are also processed in the same way.

(2) After the model training of the three base classifiers is completed, model training is carried out by using the (X1, X2, X3) obtained from the training set in the process of the model training of the base classifier as the feature input value of the logistic regression algorithm to obtain the LR classifier model, which is also called the meta-classifier.

(3) The trained meta-classifier is used to identify the three eigenvalues (Y1, Y2, Y3) which is obtained from the prediction set, and the final recognition result is obtained.

The parameters of the Stacking algorithm are set as follows: (1) XGBoost: the learning rate is 0.2, the maximum number of the regression trees that can be generated is 300, the tree depth is 5, and the sample extraction ratio is 0.8. (2) Random Forest: the maximum number of decision trees

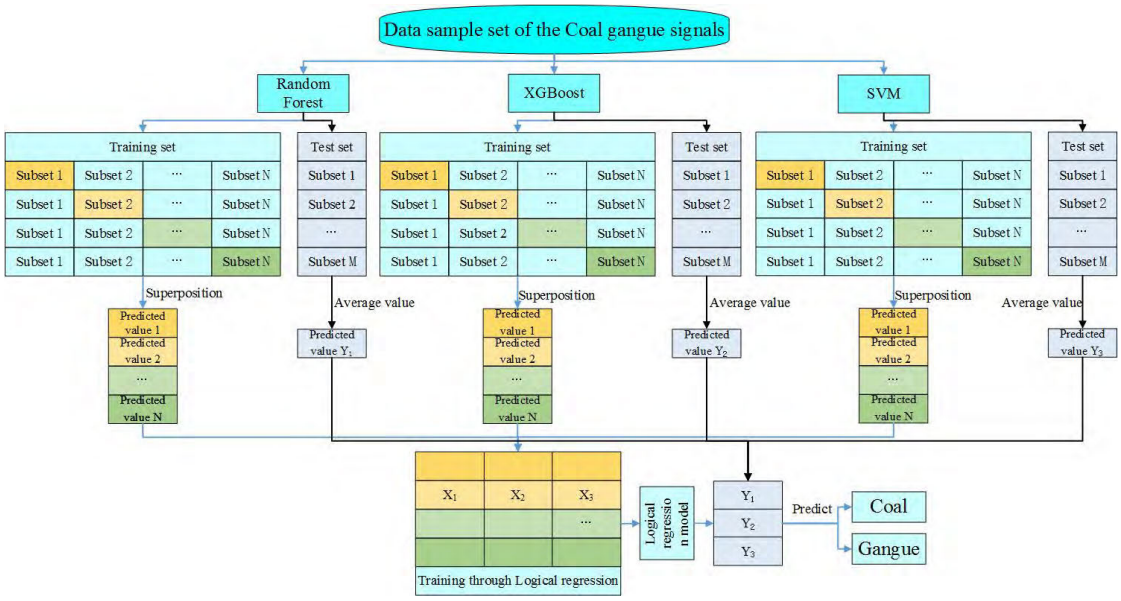

FIGURE 15. Single particle coal gangue recognition process based on Stacking integration.

TABLE 7. Recognition success rate of the stacking algorithm (%).

1	2	3	4	5	6	7	8	9	Average recognition rate	Average Time (s)
93.75	93.5	94	93.5	93	92.75	95	94	93	93.61	4.197

that can be generated is 300. The splitting evaluation standard is based on the Gini index, and the out-of-bag sample estimation is adopted. (3) Support Vector Machine: using the linear kernel function, and the penalty coefficient is 2. The remaining parameters of the XGBoost, the RF, and the SVM are set as the same with the above corresponding model settings. The penalty coefficient of the logistic regression is 8, which is also used as the meta-classifier.

The recognition feature vector of each group test signal in 2,000 groups of coal gangue impact test was also obtained. 1,600 groups of data (800 groups of coal impact and 800 groups of gangue impact) were selected to train the recognition model, and the remaining 400 groups of data were used to test the accuracy of the model. Through 9 time training and corresponding 9 time test experiments, the recognition success rate of the 400 groups of coal and gangue test data obtained is shown in Table 7.

According to the table, the average recognition success rate of the Stacking integration algorithm is 93.61%, which is 2.99% higher than the highest one 90.888,89% among random forest, XGBoost and SVM algorithms. And the highest recognition rate of the Stacking integration is 95%, if it is used in practical engineering application, it will be helpful to improve accuracy and efficiency. However, the average computing time also increased to 4.197s. Because the computational time includes training the model and test experiment in this paper, if the training model is completed in advance, the actual recognition time is very short, and the time of 4.197s is within the permissible range. Compared with six general classification algorithms, the recognition accuracy of the Stacking integration algorithm is improved by prolonging part of the computational time. By comprehensive comparison, the stacking integration algorithm based on the recognition feature vector of the intercepted signal satisfies the time effect and recognition rate, so it is more suitable for single coal gangue recognition than general classification algorithm.

VI. SINGLE PARTICLE COAL GANGUE RECOGNITION AND TWO KINDS OF SAMPLE RECOGNITION COMPARATIVE ANALYSIS BASED ON THE INTERCEPTED SIGNALS

The above 7 groups of algorithms were used to identify the coal and gangue based on the original intercepted vibration signals obtained from 2000 groups of coal gangue impact tests, and the recognition accuracy was shown in Table 8.

Compared with Tables 6-8, we can learn that each algorithm's recognition success rate by using the original intercepted signals to identify directly is higher than using the recognition feature vector of the intercepted signals. The reason is that the recognition feature extracting process lost the other features of the intercepted signals. However, because of the original intercepted signals data quantity is greater than the data quantity of the recognition feature vector of the intercepted signals, the time cost increase greatly when using

TABLE 8. Recognition success rate based on the original intercepted vibration signals (%).

Train no.	DT	RF	XGBoost	LSTM	SVM	FM	Stacking
1	84.94	95.27	95.32	76.8	92.53	52.01	97.04
2	84.3	95.15	95.2	76.93	89.73	55.71	96.55
3	82.93	94.05	94.97	77.03	90.43	61.97	97.64
4	81.75	93.92	94.95	76.24	90.45	58.9	97.08
5	82.26	94.33	95.16	76.4	91.4	51.87	96.78
6	85.83	94.69	94.93	75.95	89.52	73.23	98.12
7	83.24	95.49	95.48	75.77	90.53	59.79	97.11
8	82.2	94.98	95.08	77.02	89.84	73.33	97.38
9	80.32	93.68	95.32	76.62	88.65	69.74	97.62
Average recognition rate	83.09	94.62	95.16	76.53	90.34	61.84	97.26
Average time(s)	10.673	16.829	59.433	247.288	16.048	31.661	182.970

the same recognition algorithm to identify the coal gangue directly through the original intercepted signals.

Compared with the recognition by using Stacking integrated algorithm with the recognition feature vector of the intercepted signals, the recognition by using the DT, LSTM, SVM and FM with the original intercepted signals need the longer time but the low recognition success rate. Although the recognition success rate of the random forest algorithm with the original intercepted signals is 1.01% higher than that of Stacking integrated algorithm with the recognition feature vector of the intercepted signals, the calculate time of the former is more than 4 times of the latter. The recognition success rate of the XGBoost algorithm with the original intercepted signals is improved by 1.55% than that of Stacking integrated algorithm with the recognition feature vector of the intercepted signals, but it takes nearly 1min, which is more than 14 times of the latter. The recognition rate of Stacking integrated algorithm using the original intercepted signals is stable above 96.5%, up to 98%, but the time consumption increases to more than 3min. But with the same data sample condition, the Stacking integrated algorithm has the highest recognition rate.

Under the different social and economic situations, the coal production enterprises are facing the different pressures and therefore have the different requirements for the coal production technology and the mining rate (Mining rate: refers to the percentage of the mined raw coal in its recoverable reserves). At the same time, transportation and washing costs of coal gangue in the later stage also have some requirements for its mining rate and the proportion of coal gangue. (1) When the economic situation of the coal is poor, in order to improve the competitiveness of the enterprises, coal producers often try their best to increase the mining rate of the coal and to mine more coal (or even all coal). When gangue is identified in the process of top coal caving, it is not required to stop caving immediately. At this moment there are two options: when the mining rate of the coal is required as high as possible, but the quality of the coal is allowed to poor, there is no requirement for time, so the Stacking integrated algorithm based on the original intercepted signal can be selected for the coal gangue recognition; when the requirement for coal quality in the coal using area is lower and the requirement for time is not high, the Random Forest algorithm based on the original intercepted signal can be chosen. (2) When coal production enterprises have a large amount of coal resources and the social demand for the coal is high with good benefits, the existence of gangue will reduce the coal quality, increase the cost of transportation and washing, also the washing process will increase the cycle of the coal from production to market. At this point, when gangue is identified, the caving shall be stopped immediately, and requiring the recognition response to be extremely rapid, so the XGBoost algorithm based on the recognition feature vector of the intercepted signal can be selected for recognition. (3) When the economic situation, the demand and the benefit of the coal are at a general level, a certain proportion of gangue is allowed in top coal caving mining, such as the ratio of mixed gangue is 10%-30%. At this time, there are certain requirements for the recognition rate and recognition response time (higher recognition rate, shorter response time). At this point, the Staking integrated algorithm based on the recognition feature vector of the integrated signal can be selected for recognition. For the normal working conditions of the top coal caving, the production enterprises have the complete top coal mining, transportation, washing and sales processes, allowing some gangue mixing in the mining process to achieve the balance of the high mining rate and the low post-treatment cost. Considering the application requirements comprehensively, the Staking integrated algorithm based on the feature vectors of the integrated signals is the most suitable method to meet the usage requirements.

VII. CONCLUSIONS

The realization of unmanned automation technology in fully mechanized top-coal caving can release manpower, improve the production safety and efficiency, and reduce the mining cost. However, coal gangue recognition in the process of the fully mechanized top-coal caving has always been the bottleneck problem of the unmanned automation technology realization in fully mechanized top-coal caving. Because of the underground complex environment, more dust, less light and more noise in the top coal caving, it is very difficult to directly recognize the coal gangue interface on the working face. In order to realize the recognition of the coal gangue

interface in the complicated underground caving mining process, this paper adopts the research idea of breaking up the whole into parts and the point-to-surface research thinking, extracts the recognition problem of the single-particle coal gangue from the study of the coal gangue interface recognition on fully mechanized mining face, and puts forward a scheme of the coal gangue recognition based on the collision vibration signal between coal gangue particles and the metal plate. Based on this, the vibration test device and test system of single-particle coal gangue direct impact on the metal plate were designed and conducted independently. To simulate the random impact between any coal gangue particle and the tail beam metal plate during the top coal caving, the tests which 1,000 groups of random shape coal and 1,000 groups of random shape gangue from the random height impact on the metal plate were carried out respectively. Through the signal acquisition, signal processing and signal recognition of the 2,000 groups metal plate vibration signals, the coal gangue identification rate and calculation time are finally obtained, and the following conclusions are drawn:

(1) Aiming at the problem of the coal gangue recognition in the complex fully mechanized face, the idea of breaking up the whole into parts and the point-to-surface research thinking is put forward. The coal gangue interface recognition is disassembled into the single-particle coal gangue recognition, the multi-particle coal gangue recognition, the group-particle coal gangue recognition, and the coal gangue interface recognition based on the top coal caving characteristics, which formed the step-by-step study and reduces the difficulty of the research. This paper focuses on the recognition technology of the single-particle coal gangue. Based on the vibration signal of the metal plate, the signal processing means and the recognition classification algorithm, the recognition of the single-particle coal gangue is successfully realized, which provides research methods and foundations for the multi-particle coal gangue recognition, the group-particle coal gangue recognition, and the coal gangue interface recognition based on the top coal caving characteristics.

(2) In order to acquire the characteristics of the metal plate vibration acceleration signal which can be used to recognize the coal gangue, the standardized processing method of the signal intercepting to the test signals is presented, and 5,000 effective sample points of each group of the signal are obtained to constitute the intercepted signal. Through the traditional time-domain characteristic calculation, EMD decomposition and HAS processing to the intercepted signals, the time-frequency domain characteristics of the metal plate vibration signals when coal gangue impacts are obtained respectively. After the comparative analysis, the Variance, Peak-to-Peak value and Kurtosis index of the Intercepted signals and the energy value of the Hilbert marginal spectrum which the coal gangue impact vibration signal has the low overlap of the value range, and the energy values of the first six IMF components with the large attenuation speed and the stable attenuation, are finally determined as 10 recognition features of the coal gangue impact vibration signals, and forming the coal gangue recognition feature vector.

(3) In order to realize the identification of the coal and gangue, based on the recognition feature vector (Each group of the test signal has 10 sample points.) and 6 classification algorithms such as the DT, RF, XGBoost, LSTM, SVM and FM, 9 times recognition model trainings were conducted for 800 groups of the coal impact signals and 800 groups of the gangue impact signals respectively. And the corresponding 9 time test experiments were carried out for the remaining 200 groups of the coal impact signals and 200 groups of the gangue impact signals. Among them, the average recognition rate of RF, XGBoost and SVM is between 90% and 91%, while the average recognition rate of the other three algorithms is lower than 86.5%.

(4) In order to improve the coal gangue recognition accuracy, random forest, three algorithms with the relatively high average recognition rate, RF, XGBoost and SVM were selected as the recognition base model for the Stacking integrated algorithm. The average recognition rate of the Stacking integrated algorithm based on the recognition feature vector of the intercepted signals is 93.61%, while the highest recognition rate is 95%. The recognition accuracy is increased by more than 2.99% compared with the three groups of the base models.

(5) For the comparative analysis, the above 7 algorithms are adopted to the coal gangue recognition based on the original intercepted signals (each set of test signals has 5,000 sample points) respectively. The extraction process of the recognition feature vector greatly reduces the amount of the data calculation, but other features of the intercepted signal are lost. Compared with the recognition based on the recognition feature vector, the same algorithm based on the original intercepted signals has the higher recognition accuracy, but it's time costs have increased considerably. Among the two different recognition samples, the Stacking integrated algorithm has the highest recognition rate.

(6) The production requirements of the coal are related to the socio-economic situation, the demand for the coal, the cost of the transportation and washing, and the using place. In order to determine the best identification scheme in the application process, a recognition scheme is formulated by taking into account the two indicators of recognition accuracy and time cost. If the mining rate is required as high as possible, but there is no requirement for the coal quality, then there is no time requirement. Stacking integrated algorithm based on the original intercepted signal can be used to identify the coal gangue. If coal quality has some requirement but is not high, the requirement for time is

low, the Random Forest algorithm based on the original intercepted signal can be used to identify the coal gangue. If the caving should be stopped immediately when gangue is identified and the recognition response shall be extremely rapid, the XGBoost algorithm based on the recognition feature vector of the intercepted signal can be used for the coal gangue recognition. If a certain proportion of gangue is allowed to exist, the recognition rate must be higher and the response time must be shorter, Stacking integrated algorithm based on the intercepted signal recognition feature vector can be selected for the coal gangue recognition. Considering the requirement in the top coal caving process comprehensively, Staking integrated algorithm based on the feature vector of the intercepted signal to identify is the best.

The conclusions of this paper will provide processing methods for the non-stationary and non-linear vibration signals, provides theoretical guidance for the selection of the recognition algorithms, provide analysis ideas for the determination of the recognition features. It also provides the idea of breaking up the whole into parts and the point-to-surface research thinking for the research of the coal gangue interface recognition technology in top coal caving, as well as the research basis for the realization of the coal gangue interface recognition technology in top coal caving. However, how to further improve the recognition accuracy and reduce the operation time, and apply the recognition method to the actual top coal caving production, will be an important research goal in the future.

REFERENCES

[1] *Outline of the Thirteenth Five-Year Plan for National Economic and Social Development of the People's Republic of China*, People's Daily, Beijing, China, 2016.

[2] Q. X. Qi, Y. S. Pan, L. Y. Shu, H. Y. Li, D. Y. Jiang, S. K. Zhao, Y. H. Zou, J. F. Pan, K. J. Wang, and H. T. Li, "Theory and technical framework of prevention and control with different sources in multi-scales for coal and rock dynamic disasters in deep mining of coal mines," *J. China Coal Soc.*, vol. 43, no. 7, pp. 1801–1810, 2018. doi: 10.13225/j.cnki.jccs.2018.0660.

[3] L. J. Xu, "Research on key technology of squirrelcage selectivity separation equipment for coal and gangue underground," Ph.D. dissertation, School Mechtron. Eng., China Univ. Mining Technol., Xuzhou, China, 2012.

[4] A. Vakilin and B. K. Hebblewhite, "A new cavability assessment criterion for longwall top coal caving," *Int. J. Rock Mech. Mining Sci.*, vol. 47, pp. 1317–1329, Dec. 2010. doi: 10.1016/j.ijrmms.2010.08.010.

[5] N. E. Yasitli and B. Unver, "3D numerical modeling of longwall mining with top-coal caving," *Int. J. Rock Mech. Mining Sci.*, vol. 42, pp. 219–235, Feb. 2005. doi: 10.1016/j.ijrmms.2004.08.007.

[6] N. Zhang, C. Liu, and P. Yang, "Flow of top coal and roof rock and loss of top coal in fully mechanized top coal caving mining of extra thick coal seams," *Arabian J. Geosci.*, vol. 9, p. 465, May 2016. doi: 10.1007/s12517-016-2493-8.

[7] H. Alehossein and B. A. Poulsen, "Stress analysis of longwall top coal caving," *Int. J. Rock Mech. Mining Sci.*, vol. 47, pp. 30–41, Jan. 2010. doi: 10.1016/j.ijrmms.2009.07.004.

[8] J.-W. Zhang, J.-C. Wang, W.-J. Wei, Y. Chen, and Z.-Y. Song, "Experimental and numerical investigation on coal drawing from thick steep seam with longwall top coal caving mining," *Arabian J. Geosci.*, vol. 11, p. 96, Mar. 2018. doi: 10.1007/s12517-018-3421-x.

[9] W. Cao, J.-Q. Shi, G. Si, S. Durucan, and A. Korre, "Numerical modelling of microseismicity associated with longwall coal mining," *Int. J. Coal Geol.*, vol. 193, pp. 30–45, Jun. 2018. doi: 10.1016/j.coal.2018.04.010.

[10] A. K. Verma and D. Deb, "Numerical analysis of an interaction between hydraulic-powered support and surrounding rock strata," *Int. J. Geomech.*, vol. 13, pp. 181–192, Apr. 2013. doi: 10.1061/(ASCE)GM.1943-5622.0000190.

[11] N. B. Zhang, C. Y. Liu, X. H. Chen, and B. B. Chen, "Measurement analysis on the fluctuation characteristics of low level natural radiation from gangue," *J. China Coal Soc.*, vol. 40, no. 5, pp. 988–993, 2015. doi: 10.13225/j.cnki.jccs.2014.0776.

[12] Y. F. Wang, Y. T. Xia, and X. C. Wang, "Application on overcomplete ICA with noise in coal and rock identification of fully mechanized mining," *J. China Coal Soc.*, vol. 36, no. S1, pp. 203–206, 2011. doi: 10.13225/j.cnki.jccs.2011.s1.040.

[13] F. Q. Liu, J. S. Qian, X. H. Wang, and J. L. Song, "Automatic separation of waste rock in coal mine based on image procession and recognition," *J. China Coal Soc.*, vol. 25, no. 5, pp. 534–537, 2000. doi: 10.13225/j.cnki.jccs.2000.05.020.

[14] J. P. Sun and J. She, "Wavelet-based coal-rock image feature extraction and recognition," *J. China Coal Soc.*, vol. 38, no. 3, pp. 1900–1904, 2013. doi: 10.13225/j.cnki.jccs.2013.10.031.

[15] J. Sun and B. Su, "Coal–rock interface detection on the basis of image texture features," *Int. J. Mining Sci. Technol.*, vol. 23, no. 5, pp. 681–687, 2013. doi: 10.1016/j.ijmst.2013.08.011.

[16] J. Sun and J. She, "Coal-rock imagefeature extraction and recognition based on support vector machine," *J. China Coal Soc.*, vol. 38, no. S2, pp. 508–512, 2013. doi: 10.13225/j.cnki.jccs.2013.s2.011.

[17] H. Wei, "Identification of coal and gangue by feed-forward neural network based on data analysis," *Int. J. Coal Preparation Utilization*, vol. 39, no. 1, pp. 33–43, 2019. doi: 10.1080/19392699.2017.1290609.

[18] W. D. Wang and C. Zhang, "Separating coal and gangue using three-dimensional laser scanning," *Int. J. Mineral Process.*, vol. 694, pp. 79–84, Dec. 2017. doi: 10.1016/j.minpro.2017.10.010.

[19] A. X. He, N. Liu, and G. F. Wei, "Coal-gangue acoustic signal recognition based on sparse representation," *Appl. Mech. Materials.*, vols. 333–335, pp. 546–549, Jul. 2013. doi: 10.4028/www.scientific.net/AMM.333-335.546.

[20] Y. Liu, J. Zhou, and C. Du, "Impact crushing probability difference between coal and gangue particles based on fractal theory," *J. Central South Univ.*, vol. 45, no. 3, pp. 2935–2940, 2014.

[21] J. Zhou, Y. Liu, C. Du, and F. Wang, "Experimental study on crushing characteristic of coal and gangue under impact load," *Int. J. Coal Preparation Utilization*, vol. 36, no. 5, pp. 272–282, 2016. doi: 10.1080/19392699.2015.1114478.

[22] W. Liu, K. He, C.-Y. Liu, Q. Gao, and Y. H. Yan, "Coal-gangue interface detection based on Hilbert spectral analysis of vibrations due to rock impacts on a longwall mining machine," *Proc. Inst. Mech. Eng., C, J. Mech. Eng. Sci.*, vol. 229, no. 8, pp. 1523–1531, 2015. doi: 10.1177/0954406214543409.

[23] W. Liu, Y. Yan, and R. Wang, "Application of Hilbert–Huang transform and SVM to coal gangue interface detection," *J. Comput.*, vol. 6, no. 3, pp. 1262–1269, 2011. doi: 10.4304/jcp.6.6.1262-1269.

[24] W. Liu, "Application of Hilbert–Huang transform to vibration signal analysis of coal and gangue," *Appl. Mech. Mater.*, vols. 40–41, no. 18, pp. 995–999, 2011. doi: 10.4028/www.scientific.net/AMM.40-41.995.

[25] G.-H. Xue, X.-Y. Zhao, E.-M. Liu, W.-J. Ding, and B.-H. Hu, "Researching coal and rock character recognition based on wavelet packet frequency band energy," *Open Automat. Control Syst. J.*, vol. 6, pp. 1793–1797, 2014. doi: 10.2174/1874444301406011793.

[26] D. M. Hobson, R. M. Carter, Y. Yan, and Z. Lv, "Differentiation between coal and stone through image analysis of texture features," in *Proc. IEEE Int. Workshop Imag. Syst. Techn. (IST)*, May 2007, pp. 1–4. doi: 10.1109/IST.2007.379597.

[27] Q. Mu and J.-X. Dong, "The application of coal cleaning detection system based on embedded real-time image processing," in *Proc. 5th Int. Conf. Measuring Technol. Mechatronics Automat.*, Jan. 2013, pp. 1125–1127. doi: 10.1109/ICMTMA.2013.274.

[28] J.-K. Xu, Z.-C. Wang, W.-Z. Zhang, and Y.-P. He, "Coal-rock interface recognition based on MFCC and neural network," *Int. J. Signal Process., Image Process. Pattern Recognit.*, vol. 6, no. 4, pp. 191–200, 2013. doi: 10.3389/fpsyg.2013.00735.

[29] Z. Wang, L. Si, C. Tan, and X. Liu, "A novel approach for shearer cutting load identification through integration of improved particle swarm optimization and wavelet neural network," *Adv. Mech. Eng.*, vol. 6, Feb. 2014, Art. no. 521629. doi: 10.1155/2014/521629.

[30] L. Si, Z. Wang, X. Liu, C. Tan, J. Xu, and K. Zheng, "Multi-sensor data fusion identification for shearer cutting conditions based on parallel quasi-newton neural networks and the dempster-shafer theory," *Sensors*, vol. 15, no. 3, pp. 28772–28795, 2015. doi: 10.3390/s151128772.

[31] B. Wang, Z. Wang, and S. Zhu, "Coal-rock interface recognition based on time series analysis," in *Proc. Int. Conf. Comput. Appl. Syst. Modeling (ICCASM)*, Oct. 2010, pp. V8-356–V8-359.

[32] B. Wang, Z. Wang, and W. Z. Zhang, "Coal-rock interface recognition method based on EMD and neural network," *J. Vib., Meas. Diagnosis*, vol. 32, no. 4, pp. 586–590, 2012. doi: 10.16450./j.cnki.issn.1004-6801.2012.04.007.

[33] B. Wang, Z. Wang, and J. Xu, "A new coal-rock interface recognition method based on Hilbert marginal spectrum distribution characteristics," *J. Comput. Inf. Syst.*, vol. 8, no. 3, pp. 8137–8142, 2012.

[34] W. Hua, X. Zhao, C. Luo, G. Xue, and M. Wu, "Coal-rock interface recognition method based on dimensionless parameters and support vector machine," *Electron. J. Geotechnical Eng.*, vol. 21, no. 16, pp. 5477–5486, 2016.

[35] Y. L. Zhang and S. X. Zhang, "Analysis of coal and gangue acoustic signals based on Hilbert–Huang transformation," *J. China Coal Soc.*, vol. 35, no. 1, pp. 165–168, 2010. doi: 10.13225/j.cnki.jccs.2010.01.036.

[36] T. Y. Li, "Coal gangue image edge detection based on wavelet transform," *Appl. Mech. Mater.*, vol. 214, pp. 375–380, Nov. 2012. doi: 10.4028/www.scientific.net/AMM.214.375.

[37] Q. J. Song, X. M. Xiao, T. S. Zhang, and J. L. Wang, "Automatic control systems in top-coal caving based on acoustic wave," *Comput. Eng. Des.*, vol. 36, no. 11, pp. 3123–3127, 2015. doi: 10.16208/j.issn1000-7024.2015.11.048.

[38] Q. Song, H. Jiang, X. Zhao, and D. Li, "An automatic decision approach to coal–rock recognition in top coal caving based on MF-Score," *Pattern Anal. Appl.*, vol. 20, no. 4, pp. 1307–1315, 2017. doi: 10.1007/s10044-017-0618-7.

[39] Q. Song, H. Jiang, Q. Song, X. Zhao, and X. Wu, "Combination of minimum enclosing balls classifier with SVM in coal-rock recognition," *PLoS ONE*, Vol.12, no. 9, 2017, Art. no. e0184834. doi: 10.1371/journal.pone.0184834.

[40] D. Doua, D. Zhou, J. Yang, and Y. Zhang, "Coal and gangue recognition under four operating conditions by using image analysis and Relief-SVM," *Int. J. Preparation Utilization*, to be published. doi: 10.1080/19392699.2018.1540416.

[41] L. Li, H. Wang, and L. An, "Research on recognition of coal and gangue based on image processing," *World J. Eng.*, vol. 12, no. 3, pp. 247–254, 2015. doi: 10.1260/1708-5284.12.3.247.

[42] D. P. Tripathy and K. G. R. Reddy, "Novel methods for separation of gangue from limestone and coal using multispectral and joint color-texture features," *J. Inst. Eng. (India), Ser. D*, vol. 98, no. 1, pp. 109–117, 2017. doi: 10.1007/s40033-015-0106-4.

[43] N. Zhang and C. Liu, "Radiation characteristics of natural gamma-ray from coal and gangue for recognition in top coal caving," *Sci. Rep.*, vol. 8, no. 1, p. 190, 2018. doi: 10.1038/s41598-017-18625-y.

[44] Y. Le, Z. Lixin, D. Yongzhao, and H. Xuan, "Image recognition method of coal and coal gangue based on partial grayscale compression extended coexistence matrix," *J. Huaqiao Univ. (Natural Sci.)*, vol. 39, no. 6, pp. 906–912, 2018. doi: 10.11830/ISSN.1000-5013.201610012.

[45] H. Minamoto and S. Kawamura, "Moderately high speed impact of two identical spheres," *Int. J. Impact Eng.*, vol. 38, pp. 123–129, Feb./Mar. 2011. doi: 10.1016/j.ijimpeng.2010.09.005.

[46] T. Krijt, C. Güttler, D. Heißelmann, C. Dominik, and A. G. G. M. Tielens, "Energy dissipation in head-on collisions of spheres," *J. Phys. D, Appl. Phys.*, vol. 46, no. 43, 2013, Art. no. 435303. doi: 10.1088/0022-3727/46/43/435303.

[47] Y. Zhang and I. Sharf, "Validation of nonlinear viscoelastic contact force models for low speed impact," *J. Appl. Mech.*, vol. 76, no. 5, 2009, Art. no. 051002. doi: 10.1115/1.3112739.

[48] H. Xiao, M. J. Brennan, and Y. Shao, "On the undamped free vibration of a mass interacting with a Hertzian contact stiffness," *Mech. Res. Commun.*, vol. 38, pp. 560–564, Dec. 2011. doi: 10.1016/j.mechrescom.2011.07.012.

[49] M. R. Brake, "The effect of the contact model on the impact-vibration response of continuous and discrete systems," *J. Sound Vibrat.*, vol. 332, pp. 3849–3878, Jul. 2013. doi: 10.1016/j.jsv.2013.02.003.

[50] R. Jackson, I. Chusoipin, and I. Green, "A finite element study of the residual stress and deformation in hemispherical contacts," *J. Tribol.*, vol. 127, no. 3, pp. 484–493, 2005. doi: 10.1115/1.1843166.

[51] E. Olsson and P.-L. Larsson, "On the tangential contact behavior at elastic–plastic spherical contact problems," *Wear*, vol. 319, pp. 110–117, Nov. 2014. doi: 10.1016/j.wear.2014.07.016.

[52] J. Jamari and D. J. Schipper, "An elastic-plastic contact model of ellipsoid bodies," *Tribol. Lett.*, vol. 21, no. 3, pp. 262–271, 2006. doi: 10.1007/s11249-006-9038-3.

[53] L. Vu-Quoc, X. Zhang, and L. Lesburg, "Normal and tangential force–displacement relations for frictional elasto-plastic contact of spheres," *Int. J. Solids Struct.*, vol. 38, pp. 6455–6489, Sep. 2001. doi: 10.1016/S0020-7683(01)00065-8.

[54] R. L. Jackson, R. Green, and D. B. Marghitu, "Predicting the coefficient of restitution of impacting elastic-perfectly plastic spheres," *Nonlinear Dyn.*, vol. 60, no. 3, pp. 217–229, 2010. doi: 10.1007/s11071-009-9591-z.

[55] T. Wang, L. Wang, L. Gu, and D. Zheng, "Stress analysis of elastic coated solids in point contact," *Tribol. Int*, vol. 86, pp. 52–61, Jun. 2015. doi: 10.1016/j.triboint.2015.01.013.

[56] C. Thornton, S. J. Cummins, and P. W. Cleary, "On elastic-plastic normal contact force models, with and without adhesion," *Powder Technol.*, vol. 315, pp. 339–346, Jun. 2017. doi: 10.1016/j.powtec.2017.04.008.

[57] E. Willert, I. A. Lyashenko, and V. L. Popov, "Influence of the Tabor parameter on the adhesive normal impact of spheres in Maugis-Dugdale approximation," *Comput. Part. Mech.*, vol. 5, no. 3, pp. 313–318, 2017. doi: 10.1007/s40571-017-0170-7.

[58] X. Zhang and L. Vu-Quoc, "An accurate elasto-plastic frictional tangential force-displacement model for granular-flow simulations: Displacement-driven formulation," *J. Comput. Phys.*, vol. 225, pp. 730–752, Jul. 2007. doi: 10.1016/j.jcp.2006.12.028.

[59] Z. Wang, H. Yu, and Q. Wang, "Layer-substrate system with an imperfectly bonded interface: Spring-like condition," *Int. J. Mech. Sci*, vol. 134, pp. 315–335, Dec. 2017. doi: 10.1016/j.ijmecsci.2017.10.028.

[60] J. Xie, M. Dong, S. Li, Y. Shang, and Z. Fu, "Dynamic characteristics for the normal impact process of micro-particles with a flat surface," *Aerosol Sci. Technol.*, vol. 52, no. 2, pp. 222–233, 2017. doi: 10.1080/02786826.2017.1396440.

[61] Y. Yang, Q. Zeng, and L. Wan, "Dynamic response analysis of the vertical elastic impact of the spherical rock on the metal plate," *Int. J. Solids Struct.*, vol. 158, pp. 287–302, Feb. 2019. doi: 10.1016/j.ijsolstr.2018.09.017.

[62] Y. Yang, Q. Zeng, and L. Wan, "Contact response analysis of vertical impact between elastic sphere and elastic half space," *Shock Vib.*, vol. 2018, Nov. 2018, Art. no. 1802174. doi: 10.1155/2018/1802174.

[63] L. Lin and F. Chu, "HHT-based AE characteristics of natural fatigue cracks in rotating shafts," *Mech. Syst. Signal Process.*, vol. 26, pp. 181–189, Jan. 2012. doi: 10.1016/j.ymssp.2011.07.017.

[64] A. G. Espinosa, J. A. Rosero, J. Cusidó, L. Romeral, and J. A. Ortega, "Fault detection by means of Hilbert–Huang transform of the stator current in a PMSM with demagnetization," *IEEE Trans. Energy Convers.*, vol. 25, no. 2, pp. 312–318, Jun. 2010. doi: 10.1109/TEC.2009.2037922.

[65] T. Kalvoda and Y.-R. Hwang, "A cutter tool monitoring in machining process using Hilbert–Huang transform," *Int. J. Mach. Tools Manuf.*, vol. 50, no. 5, pp. 495–501, 2010. doi: 10.1016/j.ijmachtools.2010.01.006.

[66] J. Zhang, X. Tan, and P. Zheng, "Non-destructive detection of wire rope discontinuities from residual magnetic field images using the Hilbert–Huang transform and compressed sensing," *Sensors*, vol. 17, no. 3, p. 608, 2017. doi: 10.3390/s17030608.

[67] E. Elbouchikhi, V. Choqueuse, Y. Amirat, M. El Hachemi Benbouzid, and S. Turri, "An efficient Hilbert–Huang transform-based bearing faults detection in induction machines," *IEEE Trans. Energy Convers.*, vol. 32, no. 2, pp. 401–413, Jun. 2017. doi: 10.1109/TEC.2017.2661541.

[68] H. Zhao, M. Sun, W. Deng, and X. Yang, "A new feature extraction method based on EEMD and multi-scale fuzzy entropy for motor bearing," *Entropy*, vol. 19, no. 1, p. 14, 2017. doi: 10.3390/e19010014.

[69] A. O. Boudraa and J. C. Cexus, "EMD-based signal filtering," *IEEE Trans. Instrum. Meas.*, vol. 56, no. 6, pp. 2196–2202, Dec. 2007. doi: 10.1109/tim.2007.907967.

[70] Y. Kopsinis and S. McLaughlin, "Development of EMD-based denoising methods inspired by wavelet thresholding," *IEEE Trans. Signal Process.*, vol. 57, no. 4, pp. 1351–1362, Apr. 2009. doi: 10.1109/TSP.2009.2013885.

[71] H. Wang, Z. Liu, Y. Song, and X. Lu, "Ensemble EMD-based signal denoising using modified interval thresholding," *IET Signal Process.*, vol. 11, no. 4, pp. 452–461, Jun. 2016. doi: 10.1049/iet-spr.2016.0147.

[72] Y. Chen, C.-T. Wu, and H.-L. Liu, "EMD self-adaptive selecting relevant modes algorithm for FBG spectrum signal," *Opt. Fiber Technol.*, vol. 36, pp. 63–67, Jul. 2017. doi: 10.1016/j.yofte.2017.02.008.

[73] P. Liu, W. Huang, W. Zhang, and F. Li, "An EMD-SG algorithm for spectral noise reduction of FBG-FP static strain sensor," *IEEE Photon. Technol. Lett.*, vol. 29, no. 10, pp. 814–817, May 15, 2017. doi: 10.1109/LPT.2017.2686452.

[74] D. Looney and D. P. Mandic, "Multiscale image fusion using complex extensions of EMD," *IEEE Trans. Signal Process.*, vol. 57, no. 4, pp. 1626–1630, Apr. 2009. doi: 10.1109/TSP.2008.2011836.

[75] C. Junsheng, Y. Dejie, and Y. Yu, "A fault diagnosis approach for roller bearings based on EMD method and AR model," *Mech. Syst. Signal Process*, vol. 20, pp. 350–362, Feb. 2006. doi: 10.1016/j.ymssp.2004.11.002.

[76] J. Cheng, D. Yu, J. Tang, and Y. Yang, "Local rub-impact fault diagnosis of the rotor systems based on EMD," *Mech. Mach. Theory*, vol. 44, pp. 784–791, Apr. 2009. doi: 10.1016/j.mechmachtheory.2008.04.006.

[77] Z. Yu, F. Haghighat, B. C. M. Fung, and H. Yoshino, "A decision tree method for building energy demand modeling," *Energy Buildings*, vol. 42, no. 10, pp. 1637–1646, Oct. 2010. doi: 10.1016/j.enbuild.2010.04.006.

[78] L. Schietgat, C. Vens, J. Struyf, H. Blockeel, D. Kocev, and S. Džeroski, "Predicting gene function using hierarchical multi-label decision tree ensembles," *BMC Bioinf.*, vol. 11, p. 2, Jan. 2010. doi: 10.1186/1471-2105-11-2.

[79] H. Hong, J. Liu, D. T. Bui, B. Pradhan, T. D. Acharya, B. T. Pham, A.-X. Zhu, W. Chen, and B. B. Ahmad, "Landslide susceptibility mapping using J48 decision tree with AdaBoost, Bagging and rotation forest ensembles in the Guangchang area (China)," *Catena*, vol. 163, pp. 399–413, Apr. 2018. doi: 10.1016/j.catena.2018.01.005.

[80] S. Ragettli, J. Zhou, H. Wang, C. Liu, and L. Guo, "Modeling flash floods in ungauged mountain catchments of China: A decision tree learning approach for parameter regionalization," *J. Hydrol.*, vol. 555, pp. 330–346, Dec. 2017. (Accepted. doi: 10.1016/j.jhydrol.2017.10.031.

[81] E. S. Sankari and D. Manimegalai, "Predicting membrane protein types using various decision tree classifiers based on various modes of general PseAAC for imbalanced datasets," *J. Theor. Biol.*, vol. 435, pp. 208–217, Dec. 2017. doi: 10.1016/j.jtbi.2017.09.018.

[82] Q. Li, Y. Gu, and N.-F. Wang, "Application of random forest classifier by means of a QCM-based e-nose in the identification of Chinese liquor flavors," *IEEE Sensors J.*, vol. 17, no. 6, pp. 1788–1794, Mar. 2017. doi: 10.1109/JSEN.2017.2657653.

[83] V. Vakharia, V. K. Gupta, and P. K. Kankar, "Efficient fault diagnosis of ball bearing using ReliefF and random forest classifier," *J. Brazilian Soc. Mech. Sci. Eng.*, vol. 39, pp. 2969–2982, Aug. 2017. doi: 10.1007/s40430-017-0717-9.

[84] M. Lu, S. Sadiq, D. J. Feaster, and H. Ishwaran, "Estimating individual treatment effect in observational data using random forest methods," *J. Comput. Graph. Statist.*, vol. 27, no. 1, pp. 209–219, 2017. doi: 10.1080/10618600.2017.1356325.

[85] A. Jog, A. Carass, S. Roy, D. L. Pham, and J. L. Prince, "Random forest regression for magnetic resonance image synthesis," *Med. Image Anal.*, vol. 35, pp. 475–488, Jan. 2017. doi: 10.1016/j.media.2016.08.009.

[86] P. T. Noi and M. Kappas, "Comparison of random forest, *k*-nearest neighbor, and support vector machine classifiers for land cover classification using sentinel-2 imagery," *Sensors*, vol. 18, no. 1, p. 18, 2018. doi: 10.3390/s18010018.

[87] D. Zhang, L. Qian, B. Mao, C. Huang, B. Huang, and Y. Si, "A data-driven design for fault detection of wind turbines using random forests and XGboost," *IEEE Access*, vol. 6, pp. 21020–21031, 2018. doi: 10.1109/ACCESS.2018.2818678.

[88] W. Chen, K. Fu, J. Zuo, X. Zheng, T. Huang, and W. Ren, "Radar emitter classification for large data set based on weighted-xgboost," *IET Radar Sonar Navigat.*, vol. 11, no. 8, pp. 1203–1207, 2017. doi: 10.1049/iet-rsn.2016.0632.

[89] J. Zhong, Y. Sun, W. Peng, M. Xie, J. Yang, and X. Tang, "XGBFEMF: An XGBoost-based framework for essential protein prediction," *IEEE Trans. Nanobiosci.*, vol. 17, no. 3, pp. 243–250, Jul. 2018. doi: 10.1109/TNB.2018.2842219.

[90] Y. Zhou, T. Li, J. Shi, and Z. Qian, "A CEEMDAN and XGBOOST-based approach to forecast crude oil prices," *Complex.*, vol. 2019, Feb. 2019, Art. no. 4392785. doi: 10.1155/2019/4392785.

[91] M. Wöllmer, B. Schuller, F. Eyben, and G. Rigoll, "Combining long short-term memory and dynamic Bayesian networks for incremental emotion-sensitive artificial listening," *IEEE J. Sel. Topics Signal Process.*, vol. 4, no. 5, pp. 867–881, Oct. 2010. doi: 10.1109/JSTSP.2010.2057200.

[92] X. Ma, Z. Tao, Y. Wang, H. Yu, and Y. Wang, "Long short-term memory neural network for traffic speed prediction using remote microwave sensor data," *Transp. Res. C, Emerg. Technol.*, vol. 54, pp. 187–197, May 2015. doi: 10.1016/j.trc.2015.03.014.

[93] J. Zhang, Y. Zhu, X. Zhang, M. Ye, and J. Yan, "Developing a long short-term memory (LSTM) based model for predicting water table depth in agricultural areas," *J. Hydrol.*, vol. 561, pp. 918–929, Jun. 2018. doi: 10.1016/j.jhydrol.2018.04.065.

[94] X. Li, L. Peng, X. Yao, S. Cui, Y. Hu, C. You, and T. Chi, "Long short-term memory neural network for air pollutant concentration predictions: Method development and evaluation," *Environ. Pollut.*, vol. 231, pp. 997–1004, Dec. 2017. doi: 10.1016/j.envpol.2017.08.114.

[95] P. Rodriguez, G. Cucurull, J. Gonzàlez, J. M. Gonfaus, K. Nasrollahi, T. B. Moeslund, and F. X. Roca, "Deep pain: Exploiting long short-term memory networks for facial expression classification," *IEEE Trans. Cybern.*, to be published. doi: 10.1109/TCYB.2017.2662199.

[96] S. M. Erfani, S. Rajasegarar, S. Karunasekera, and C. Leckie, "High-dimensional and large-scale anomaly detection using a linear one-class SVM with deep learning," *Pattern Recognit.*, vol. 58, pp. 121–134, Oct. 2016. doi: 10.1016/j.patcog.2016.03.028.

[97] X. Zhang, Y. Liang, and J. Zhou, "A novel bearing fault diagnosis model integrated permutation entropy, ensemble empirical mode decomposition and optimized SVM," *Measurement*, vol. 69, pp. 164–179, Jun. 2015. doi: 10.1016/j.measurement.2015.03.017.

[98] L. Sørensen, M. Nielsen, and A. D. N. Initiative, "Ensemble support vector machine classification of dementia using structural MRI and mini-mental state examination," *J. Neurosci. Methods*, vol. 302, pp. 66–74, May 2018. doi: 10.1016/j.jneumeth.2018.01.003.

[99] K. Y. Bae, H. S. Jang, and D. K. Sung, "Hourly solar irradiance prediction based on support vector machine and its error analysis," *IEEE Trans. Power Syst.*, vol. 32, no. 2, pp. 935–945, Mar. 2017. doi: 10.1109/TPWRS.2016.2569608.

[100] S. U. Jan, Y. D. Lee, J. Shin, and I. Koo, "Sensor fault classification based on support vector machine and statistical time-domain features," *IEEE Access*, vol. 5, pp. 8682–8690, 2017. doi: 10.1109/ACCESS.2017.2705644.

[101] J. Zeng, D. Lu, Y. Zhao, Z. Zhang, W. Qiao, and X. Gong, "Wind turbine fault detection and isolation using support vector machine and a residual-based method," in *Proc. Amer. Control Conf.*, Jun. 2013, pp. 3661–3666. doi: 10.1109/ACC.2013.6580398.

[102] S. Wang, C. Li, K. Zhao, and H. Chen, "Learning to context-aware recommend with hierarchical factorization machines," *Inf. Sci.*, vols. 409–410, pp. 121–138, Oct. 2017. doi: 10.1016/j.ins.2017.05.015.

[103] W. Pan, Z. Liu, Z. Ming, H. Zhong, X. Wang, and C. Xu, "Compressed knowledge transfer via factorization machine for heterogeneous collaborative recommendation," *Knowl.-Based Syst.*, vol. 85, pp. 234–244, Sep. 2015. doi: 10.1016/j.knosys.2015.05.009.

[104] W. Guo, S. Wu, L. Wang, and T. Tan, "Personalized ranking with pairwise factorization machines," *Neurocomputing*, vol. 214, pp. 191–200, Nov. 2016. doi: 10.1016/j.neucom.2016.05.074.

[105] C. Yang, Y. Yao, Z. Chen, and B. Xia, "Analysis on cache-enabled wireless heterogeneous networks," *IEEE Trans. Wireless Commun.*, vol. 15, no. 1, pp. 131–145, Jan. 2016. doi: 10.1109/TWC.2015.2468220.

[106] P. Xu, "The study of online classification and recognition algorithm for BCI based on motor imagery," M.S. thesis, School Life Sci. Technol., Univ. Electron. Sci. Technol. China, Sichuan Sheng, China, 2017.

[107] B. B. Wang, "The study of the hierarchical prediction of Zhejiang mobile corporation customer churn based on stacking ensemble learning," M.S. thesis, School Statist. Math., ZheJiang GongShang Univ., Zhejiang Sheng, China, 2018.

[108] Z. A. Chen, "Research of information extraction algorithm on sentiment analysis of household appliances enterprises network reviews," M.S. thesis, School Inf. Softw. Eng., Univ. Electron. Sci. Technol. China, Sichuan Sheng, China, 2015.
[109] F. F. You, "The RF-stacking model with under-sampling—Prediction for semiconductor yield," M.S. thesis, School Statist., Fac. Econ. Manage., East China Normal Univ., Shanghai, China, 2018.
[110] F. Wan, "Study on the user background analysis algorithm based on Web text," M.S. thesis, School Comput. Sci. Eng., Univ. Electron. Sci. Technol. China, Sichuan Sheng, China, 2018.
[111] P. C. Li, "A multi-factor stock selection model based on seven algorithms such as stacking random forest GBDT SVM Adaboost and others," M.S. thesis, School Finance, ZheJiang GongShang Univ., Zhejiang Sheng, China, 2018.
[112] Y. Chen, M.-L. Wong, and H. Li, "Applying ant colony optimization to configuring stacking ensembles for data mining," *Expert Syst. Appl.*, vol. 41, no. 6, pp. 2688–2702, 2014. doi: 10.1016/j.eswa.2013.10.063.

YANG YANG received the B.E. degree in machine design and automation from the Shandong University of Science and Technology, in 2015, where he is currently pursuing the Ph.D. degree. His research interests include contact mechanics, coal-gangue interface recognition, signal processing, mechanical design electromechanical integration, and intelligent control.

QINGLIANG ZENG received the Ph.D. degree in machine design and theory from the China University of Mining and Technology, in 2000. He is currently a Professor with the Shandong University of Science and Technology and Shandong Normal University. He has participated more than 40 projects funded by the National Sci-Tech Support Plan, National 863 Program, and Natural Science Foundation of China. He published more than 90 papers as the principle person. His research interests include electromechanical integration, condition monitoring and fault diagnosis, and virtual prototype.

GUANGJUN YIN received the B.E. degree in machine design and automation from the Shandong University of Science and Technology, in 2016, where he is currently pursuing the master's degree.

LIRONG WAN received the Ph.D. degree from the Shandong University of Science and Technology, in 2008, where she is currently a Professor. Her research interests include virtual prototype, concurrent engineering, computer integrated manufacturing, electromechanical integration, and hydraulic transmission and control.